PhD

PROGRAM IN TRANSLATIONAL AND MOLECULAR MEDICINE

DIMET

Biological camouflage imparts cell-like activity to injectable particle: the Leukolike system

Coordinator: Prof. Andrea Biondi

Tutor: Prof. Massimo Masserini

Dr. Nicoletta Quattrocchi

Matr. No. 079215

XXIII CYCLE

ACADEMIC YEAR

2009-2010

“A tree is known by its fruit”

INDEX

11. Peer, D. and R. Margalit, *Fluoxetine and reversal of multidrug resistance.* Cancer Lett, 2006. 237(2): p. 180-7. 53

12. Torchilin, V.P., *Recent advances with liposomes as pharmaceutical carriers.* Nat Rev Drug Discov, 2005. 4(2): p. 145-60. 53

13. Reddy, L.H., *Drug delivery to tumours: recent strategies.* J Pharm Pharmacol, 2005. 57(10): p. 1231-42. 53

14. Allen, T.M., *Long-circulating (sterically stabilized) liposomes for targeted drug delivery.* Trends Pharmacol Sci, 1994. 15(7): p. 215-20. 53

15. Maeda, M., et al., *Sustained release of human growth hormone (hGH) from collagen film and evaluation of effect on wound healing in db/db mice.* J Control Release, 2001. 77(3): p. 261-72. 53

16. Stolnik, S., et al., *Surface modification of poly(lactide-co-glycolide) nanospheres by biodegradable poly(lactide)-poly(ethylene glycol) copolymers.* Pharm Res, 1994. 11(12): p. 1800-8. 53

17. Gref, R., et al., *Biodegradable long-circulating polymeric nanospheres.* Science, 1994. 263(5153): p. 1600-3. 53

18. Gabizon, A.A., *Pegylated liposomal doxorubicin: metamorphosis of an old drug into a new form of chemotherapy.* Cancer Invest, 2001. 19(4): p. 424-36. 54

19. Boman, N.L., et al., *Liposomal vincristine which exhibits increased drug retention and increased circulation longevity cures mice bearing P388 tumors.* Cancer Res, 1994. 54(11): p. 2830-3. 54

20. Gabizon, A., et al., *Prolonged circulation time and enhanced accumulation in malignant exudates of doxorubicin encapsulated in polyethylene-glycol coated liposomes.* Cancer Res, 1994. 54(4): p. 987-92. 54

21. Veronese, F.M. and G. Pasut, *PEGylation, successful approach to drug delivery.* Drug Discov Today, 2005. 10(21): p. 1451-8. 54

22. Grayson, S.M. and W.T. Godbey, *The role of macromolecular architecture in passively targeted polymeric carriers for drug and gene delivery.* J Drug Target, 2008. 16(5): p. 329-56. 54

23. Ferrari, M., *Frontiers in cancer nanomedicine: directing mass transport through biological barriers.* Trends Biotechnol, 2010. 28(4): p. 181-8. 54

24. Muller, R.H., et al., *Phagocytic uptake and cytotoxicity of solid lipid nanoparticles (SLN) sterically stabilized with poloxamine 908 and poloxamer 407.* J Drug Target, 1996. 4(3): p. 161-70. 54

25. ten Tije, A.J., et al., *Pharmacological effects of formulation vehicles : implications for cancer chemotherapy.* Clin Pharmacokinet, 2003. 42(7): p. 665-85. 54

26. Katragadda, S., et al., *Role of efflux pumps and metabolising enzymes in drug delivery.* Expert Opin Drug Deliv, 2005. 2(4): p. 683-705. .55

27. Bassingthwaighte, J.B., C.Y. Wang, and I.S. Chan, *Blood-tissue exchange via transport and transformation by capillary endothelial cells.* Circ Res, 1989. 65(4): p. 997-1020. 55

28. Silva, G.A., *Nanotechnology approaches to crossing the blood-brain barrier and drug delivery to the CNS.* BMC Neurosci, 2008. 9 Suppl 3: p. S4. 55

29. Jang, S.H., et al., *Drug delivery and transport to solid tumors.* Pharm Res, 2003. 20(9): p. 1337-50. 55

30. Nies, A.T., *The role of membrane transporters in drug delivery to brain tumors.* Cancer Lett, 2007. 254(1): p. 11-29. 55

31. Khansari, D.N., A.J. Murgo, and R.E. Faith, *Effects of stress on the immune system.* Immunol Today, 1990. 11(5): p. 170-5. 55

32. Kushner, I., *The phenomenon of the acute phase response.* Ann N Y Acad Sci, 1982. 389: p. 39-48.....55

33. Nilsson, B., et al., *Can cells and biomaterials in therapeutic medicine be shielded from innate immune recognition?* Trends in immunology, 2010. 31(1): p. 32-38.....55

34. Andersson, J., et al., *Binding of C3 fragments on top of adsorbed plasma proteins during complement activation on a model biomaterial surface.* Biomaterials, 2005. 26(13): p. 1477-85.....55

35. Owens, D.E., 3rd and N.A. Peppas, *Opsonization, biodistribution, and pharmacokinetics of polymeric nanoparticles.* Int J Pharm, 2006. 307(1): p. 93-102. 56

36. Butcher, E.C., *Leukocyte-endothelial cell recognition: three (or more) steps to specificity and diversity.* Cell, 1991. 67(6): p. 1033-6. 56

37. Springer, T.A., *Traffic signals for lymphocyte recirculation and leukocyte emigration: the multistep paradigm.* Cell, 1994. 76(2): p. 301-14. 56

38. Ley, K., et al., *Getting to the site of inflammation: the leukocyte adhesion cascade updated.* Nat Rev Immunol, 2007. 7(9): p. 678-89. 56

39. Cook-Mills, J.M. and T.L. Deem, *Active participation of endothelial cells in inflammation.* J Leukoc Biol, 2005. 77(4): p. 487-95. 56

40. Wittchen, E.S., et al., *Trading spaces: Rap, Rac, and Rho as architects of transendothelial migration.* Curr Opin Hematol, 2005. 12(1): p. 14-21. ..56

41. Marlin, S.D. and T.A. Springer, *Purified intercellular adhesion molecule-1 (ICAM-1) is a ligand for lymphocyte function-associated antigen 1 (LFA-1).* Cell, 1987. 51(5): p. 813-9. 56

42. Alon, R., et al., *The integrin VLA-4 supports tethering and rolling in flow on VCAM-1.* J Cell Biol, 1995. 128(6): p. 1243-53. 56

43. Sans, E., E. Delachanal, and A. Duperray, *Analysis of the roles of ICAM-1 in neutrophil transmigration using a reconstituted mammalian cell expression model: implication of ICAM-1 cytoplasmic domain and Rho-dependent signaling pathway.* J Immunol, 2001. 166(1): p. 544-51. 57

44. Shaw, S.K., et al., *Coordinated redistribution of leukocyte LFA-1 and endothelial cell ICAM-1 accompany neutrophil transmigration.* J Exp Med, 2004. 200(12): p. 1571-80. 57

45. Ronald, J.A., et al., *Differential regulation of transendothelial migration of THP-1 cells by ICAM-1/LFA-1 and VCAM-1/VLA-4.* J Leukoc Biol, 2001. 70(4): p. 601-9. 57

46. Kishimoto, T.K., et al., *The leukocyte integrins.* Adv Immunol, 1989. 46: p. 149-82. 57

47. Heit, B., P. Colarusso, and P. Kubes, *Fundamentally different roles for LFA-1, Mac-1 and alpha4-integrin in neutrophil chemotaxis.* J Cell Sci, 2005. 118(Pt 22): p. 5205-20. 57

48. Burns, A.R., et al., *Neutrophil transendothelial migration is independent of tight junctions and occurs preferentially at tricellular corners.* J Immunol, 1997. 159(6): p. 2893-903. 57

49. Wang, S., et al., *Venular basement membranes contain specific matrix protein low expression regions that act as exit points for emigrating neutrophils.* J Exp Med, 2006. 203(6): p. 1519-32. 57

50. Yang, L., et al., *Endothelial cell cortactin coordinates intercellular adhesion molecule-1 clustering and actin cytoskeleton remodeling during polymorphonuclear leukocyte adhesion and transmigration.* J Immunol, 2006. 177(9): p. 6440-9.....57

51. Tiruppathi, C., et al., *Role of Ca2+ signaling in the regulation of endothelial permeability.* Vascul Pharmacol, 2002. 39(4-5): p. 173-85.....58

52. Thompson, P.W., A.M. Randi, and A.J. Ridley, *Intercellular adhesion molecule (ICAM)-1, but not ICAM-2, activates RhoA and stimulates c-fos and rhoA transcription in endothelial cells.* J Immunol, 2002. 169(2): p. 1007-13. 58

53. Barreiro, O., et al., *Dynamic interaction of VCAM-1 and ICAM-1 with moesin and ezrin in a novel endothelial docking structure for adherent leukocytes.* J Cell Biol, 2002. 157(7): p. 1233-45.....58

54. Engelhardt, B. and H. Wolburg, *Mini-review: Transendothelial migration of leukocytes: through the front door or around the side of the house?* Eur J Immunol, 2004. 34(11): p. 2955-63. 58

55. Carman, C.V. and T.A. Springer, *A transmigratory cup in leukocyte diapedesis both through individual vascular endothelial cells and between them.* J Cell Biol, 2004. 167(2): p. 377-88. 58

56. Stan, R.V., *Endothelial stomatal and fenestral diaphragms in normal vessels and angiogenesis.* J Cell Mol Med, 2007. 11(4): p. 621-43.....58

57. Millan, J., et al., *Lymphocyte transcellular migration occurs through recruitment of endothelial ICAM-1 to caveola- and F-actin-rich domains.* Nat Cell Biol, 2006. 8(2): p. 113-23.....58

58. Mamdouh, Z., et al., *Targeted recycling of PECAM from endothelial surface-connected compartments during diapedesis.* Nature, 2003. 421(6924): p. 748-53. 58

59. Mamdouh, Z., G.E. Kreitzer, and W.A. Muller, *Leukocyte transmigration requires kinesin-mediated microtubule-dependent membrane trafficking from the lateral border recycling compartment.* J Exp Med, 2008. 205(4): p. 951-66. 59

60. Phillipson, M., et al., *Intraluminal crawling of neutrophils to emigration sites: a molecularly distinct process from adhesion in the recruitment cascade.* J Exp Med, 2006. 203(12): p. 2569-75. 59

61. Phillipson, M., et al., *Endothelial domes encapsulate adherent neutrophils and minimize increases in vascular permeability in paracellular and transcellular emigration.* PLoS One, 2008. 3(2): p. e1649. 59

62. Cinamon, G., et al., *Chemoattractant signals and beta 2 integrin occupancy at apical endothelial contacts combine with shear stress signals to promote transendothelial neutrophil migration.* J Immunol, 2004. 173(12): p. 7282-91. 59

63. Yang, L., et al., *ICAM-1 regulates neutrophil adhesion and transcellular migration of TNF-alpha-activated vascular endothelium under flow.* Blood, 2005. 106(2): p. 584-92. 59

64. Nwariaku, F.E., et al., *NADPH oxidase mediates vascular endothelial cadherin phosphorylation and endothelial dysfunction.* Blood, 2004. 104(10): p. 3214-20. 59

65. Ferreira, A.M., et al., *Interleukin-1beta reduces transcellular monocyte diapedesis and compromises endothelial adherens junction integrity.* Microcirculation, 2005. 12(7): p. 563-79.....59

66. Carman, C.V., et al., *Transcellular diapedesis is initiated by invasive podosomes.* Immunity, 2007. 26(6): p. 784-97.....59

67. Cho, K., et al., *Therapeutic nanoparticles for drug delivery in cancer.* Clin Cancer Res, 2008. 14(5): p. 1310-6. 60

68. Jain, R.K., *Transport of molecules, particles, and cells in solid tumors.* Annu Rev Biomed Eng, 1999. 1: p. 241-63. 60

Chapter 1

INTRODUCTION

Drug delivery

The general concept of drug delivery

The current focus in development of cancer therapies is on targeted drug delivery to increase accumulation of an active chemotherapeutic agent at a desired site of action while sparing the normal tissues, through spontaneous or induced targeting.

The therapeutic agents currently used, indeed, are able to specifically and actively interfere with the pathological processes or abnormal biological pathways only after selective accumulation at the disease sites. However, independently by the route of administration, the distribution within the body of the therapeutic agents is related to their ability to cross, before reaching the site of action, several biological barriers, such as other organs, cells and intracellular compartments where they can be inactivated or express undesirable effects. Consequently, since a great amount of it is wasted in normal tissues, in order to achieve a required effective concentration at the site of interest, the drug is commonly administered in large quantities.

To improve drug concentration in the targeted tissues, several approaches have been suggested, including the association of the drug to carrier systems, named drug delivery systems (DDS).

Distinct techniques of device fabrication at both the micro- and nano-scale are currently used to develop devices used as DDS [1] to improve the effectiveness of the pharmaceutical agent administrations. Several DDS have been developed in such ways that the drug of interest is typically encapsulated, entrapped, or adsorbed on their matrixes. The DDS so far used are commonly constituted by polymer conjugates, polymeric microparticles, lipid-based carriers such as liposomes (Figure 1) and micelles, dendrimers, gold, silicon, silica particles and carbon nanotubes, that are all classified as good biomaterials because of their high biodegradability and biocompatibility.

A large piece of work has been done using liposomes as DDS, which has led to several marketed formulations so far. For instance, the liposomal formulation of Amphotericin B, which is the leading compound in the treatment of leishmaniasis is today the more efficient treatment against this parasite and other fungal infections.

Together with liposomes, polymer particles were developed as DDS to improve the efficacy of the associated drug thanks to a better control of its biodistribution toward the diseased organ or cells and to their faculty to overcome biological barriers [2].

The primary function of the DDS is to enhance the drug therapeutic efficacy by improving the pharmacological properties of a conventional free drug such as poor solubility, loss of activity immediately after administration and premature enzymatic degradation, unfavorable pharmacokinetics, poor biodistribution and lack of selectivity for target tissues [3]. However the ideal DDS must also take into consideration a different number of needs, ranging from

biocompatibility and ease of functionalization until to the effective delivery of the drugs. Moreover an ideal DDS should own the ability to simultaneously (i) alter the pharmacokinetic and biodistribution of the coupled drug, (ii) act as drug reservoirs and (iii) guarantee a sustained release after reaching the tissue where the drug is needed [3].

To date, some DDS have demonstrated enhanced efficacy for numerous drugs compared with conventional formulations. Indeed, the biological activity of the drug associated with the DDS is generally improved, whereas the side effects due to their toxicity are reduced thanks to a better control of the biodistribution [4]. The improved efficacy can also be explained by a higher stability of the drug in biological media and ability to overcome biological barriers. However, the main limitation of these systems remains the full control of their biodistribution because they still lack precise targeting specificities.

A site specific drug targeting, indeed, will be advantageous because the consistent reduction of the quantity of the administered drug as well as of the negative side effects on non-target areas.

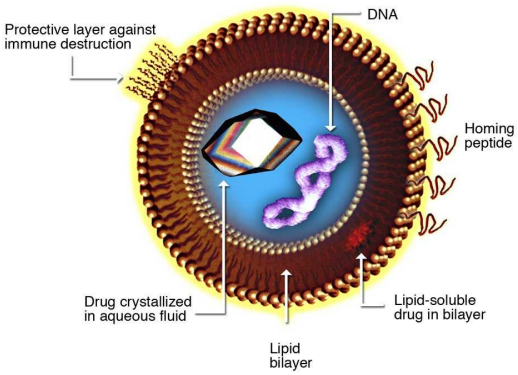

Figure 1. Schematic of a multifunctionalized DDS showing a liposome delivering an encapsulated drug, functionalized with a homing peptide for the specific site targeting and protecting molecules to ensure prolonged circulation by escaping the immune system. *(www.pratt.duke.edu)*

Targeted drug delivery: the passive and active targeting

One of the benefits expected by using a DDS is the specific delivery of the drug payload at the target site. There are two main methods for achieving the target drug delivery: the passive and the active way.

The passive targeting is accomplished by taking advantages from the characteristic features of the tumor biology. The drug-loaded DDS passively reach the target organ by exploiting the enhanced permeability and retention (EPR) effect, which constitutes the basis for the selective targeting of drugs to the site of solid tumors [5]. The EPR effect is the mostly observed in inflamed tissues and solid tumors where the tumor blood vessels are dilated and leaky, constituted by endothelial cells not well organized that show large fenestrations, ranging from 100 nm to 10 µm [6-8]. These anatomical and functional abnormalities result in a massive leakage of blood plasma constituents, including macromolecules and circulating DDS that can extravasate into the tumor mass. Furthermore the poor lymphatic

drainage and the slow venous return in the tumor tissue allow blood components to accumulate and be retained in the tumor interstitium [9]. Although passive targeting approaches represent the base of medical therapy, they encounter several limitations: some DDS cannot diffuse efficiently within a tumor, while the random nature of the approach makes it unable to efficiently control the process. The loss of control can induce multiple-drug resistance (MDR), a condition associated to the failure of chemotherapy treatments that induce the cancer cells to develop resistance towards one or more drugs. At the base of the MDR there is the over-expression, on the cancer cell surface, and activation of transporter proteins that usually remove the drugs diffused into the cells. As consequence their expelling function, the drug therapeutic effect is lowered [10, 11] while the tumor cells develop resistance to different drugs.

Nonetheless the passive strategy is restrained because not all the tumors exhibit the EPR effect, and eventually the vessel permeability cannot be the same all through a single tumor.

In order to overcome the limitations of the passive targeting, the tumor intracellular uptake of the DDS, after extravasation, can be enhanced through active targeting that demands a receptor-mediated recognition. For this purpose, targeting moieties such as ligands, molecules that bind to specific receptors on the cell surface, can be conjugated to the surface of the DDS by using different conjugation chemistries [12].

After EPR-based accumulation, the DDS will recognize and bind target cells through ligand–receptor interactions. The bound DDS will be internalized and the drug released inside the cell [13].

In the active targeting method it is important that the targeting ligand selectively binds to receptors exclusively expressed on the tumor cell surface. However, sometimes it can be advantageous to target the DDS to non-internalizing receptors so that cells missing the target receptor can be killed through drug release at the surface of the closer cells, where DDS can bind [14].

However, to date, there are still significant doubts about the relative contributions of active against passive targeting of DDS. It is not really clear if the active ligand targeting increases only the cellular internalization without affecting the total DDS accumulation in the tumor mass, or if it raises both of them.

The efficacy of drug targeting thus depends on different parameters: the size of the target, blood flow through it, number of binding sites for the targeted drug/DDS within the target site, number and affinity of targeting moieties on the DDS.

However, it is well known that both passive and active targeting require DDS to be long-circulating so that they can stay in the blood circulation for long periods in order to provide a sufficient level of accumulation at the target. Moreover,

DDS circulation in the blood and its importance for drug delivery

One of the key properties of long-circulating DDS is their longevity in the blood, for both passive and active targeting. The reasons for making long-circulating DDS are several, but the most important is to maintain a required level of a therapeutic agent in the blood for an extended time, so that long-circulating DDS can slowly accumulate in pathological sites with affected and leaky vasculature [15]. Moreover,

the prolonged circulation can help to achieve a better targeting effect by increasing the time for the interaction between the DDS and the target due to a larger number of passages through the target.

The most usual way to keep DDS in the blood long enough is to "mask" them by modifying (grafting) their surface with water-soluble polymers constituted by well-solvated and flexible chains, such as polyethylene glycol (PEG) (Figure 2) [16, 17]. Hydrophilic polymers have been shown to protect individual molecules and solid particulates from interaction with different solutes. This phenomenon, known as "steric stabilization", relates to the stability of various aqueous dispersions and helps to protect drugs and DDS from undesirable interactions with components of the biological environment. In particular, PEG sterically hinders and reduces the interactions of blood proteins (opsonins) with DDS surface. By preventing DDS interaction with opsonins it slows their fast capture and clearance by the phagocytic cells of the reticuloendothelial system (RES). Moreover, the mechanisms of preventing opsonization through PEG by enhancing repulsive interactions between the polymer and the opsonins, also increases the DDS hydrophilicity by shielding its surface charges [18].

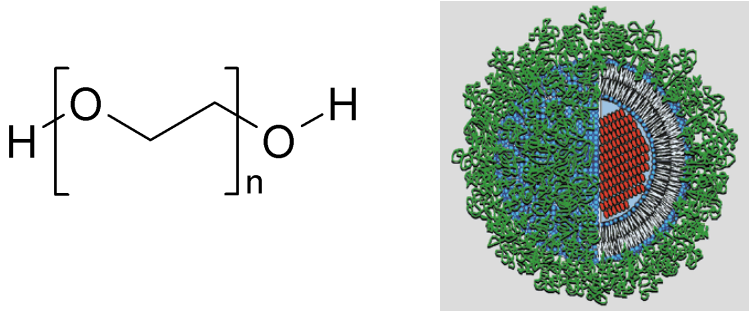

Figure 2. On the left, the molecular structure of PEG (left). On the right, a stealth liposome coated with PEG (green). (*www.life-enhancement.com)*

Advantages and disadvantages of PEGylation

Although quite few polymers have been tried as steric protectors for DDS, the majority of research on long-circulating drugs and DDS was performed by using PEG especially because of its very attractive properties: excellent solubility in aqueous solutions due to the ability to bind many water molecules, high flexibility of its polymer chains, very low toxicity, immunogenicity and antigenicity, minimum influence on specific biological properties of modified active agents, reduced accumulation in the RES and improvement of the DDS pharmacokinetics.

As a result, PEG-coated and other long-circulating DDS were prepared containing a variety of anticancer agents, such as doxorubicin (DOX), adriamycin and vincristine [19, 20]. The biggest success was achieved with PEG-liposome-incorporated DOX, which has already demonstrated very good clinical results.

However, the pharmacokinetics of PEG-coated DDS is determined by the density and the conformation of the surface-projected polymers. Usually the projection of the polymer chains assume a brush-like configuration that avoids the immediate interaction with the complement system and the following sequestration from macrophages. At a lower critical surface density, the polymer chains assume a mushroom-like configuration (Figure 3) in which the DDS surface is not completely covered and the PEG-shielded DDS has a shorter circulation time due to a faster complement activation.

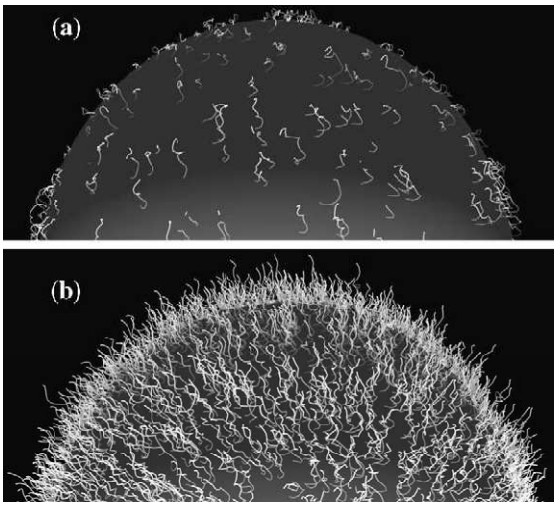

Figure 3. Schematic diagrams of PEG configurations on a DDS. In (a), the low surface coverage of PEG chains leads to the "mushroom" configuration where most of the chains are located closer to the particles surface. In (b), the high surface coverage and lack of mobility of the PEG chains leads to the "brush" configuration where most of the chains are extended away from the surface [35].

The effect of PEG surface coating on the pharmacokinetics of DDS was reported in 1994 by Gref et al. The authors showed that 66% of the uncoated DDS were cleared away by the liver already 5 minutes after injection, while less than 30% of the PEG-shielded DDS were removed by the liver after 2 h [17].

Therefore, the majority of biomedical DDS in advanced clinical trials or on the market, approved by the Food and Drug Administration, are PEG-containing products [21].

However the biocompatibility and the stealth behavior of PEG are influenced by some of its structural parameters like the molecular mass and the polydispersity of the polymer. PEG used in medical and pharmaceutical applications has a molecular mass that ranges from 400 Da to about 50 kDa. PEG with low moleclar masses, from 1 kDa to 5 kDa, is often used to avoid elimination by the RES, to reduce enzymatic degradation and to hide cationic charges. PEG with a molar mass ranging from 20 kDa to 50 kDa is frequently adopted to avoid

the fast renal clearance of the drugs by increasing the size of the drug carriers above the renal clearance threshold [22].

The PEG molecular mass also determines other polymer limitations including the non-biodegradability and the toxicity at the cellular level that causes the cellular membrane fusion and tissue vacuolization. The toxic effect is in inverse proportion to the PEG molecular mass: the oxidative degradation decreases while increasing the molecular mass. Nonetheless the molecular mass should not exceed the renal clearance threshold in order to allow a complete elimination of the polymer and to prevent a liver accumulation [21].

Additionally, PEG not only tends to shield the DDS from the immune system but also the targeting agents from their target site, reducing the probability of a successful recognition. Therefore, to date, no DDS with a biomolecular targeting strategy has received a regulatory approval [23].

Biological barriers to drug delivery

To date, through rational drug design, very specific drugs have been developed with molecular properties that allow the optimal interaction with the specific macromolecules (receptors, enzymes) able to mediate their pharmacological effects. However, although their delivery to the site of action can be improved by incorporating them into a DDS, a major challenge in drug delivery is to circumvent all the biological barriers, such as intestinal mucosa, RES [24], thrombocytes and erythrocytes [25], attack by lytic enzymes [26], crossing of the endothelial wall [27] or blood brain barrier (BBB) [28], diffusion in perivascular tissue against interstitial and osmotic pressure [29] and

entry into the cell cytoplasm through the extracellular lipid bilayer [30], that often prevent the potential clinical use of drugs by avoiding the reaching of their site action.

The biological barriers to drug delivery can basically be divided into epithelial, elimination and target cell barriers.

The epithelial barriers that restrict permeability of drugs to the systemic circulation include the intestinal epithelium, oral epithelium and dermal epithelium that act as both physical and biochemical barriers. As physical barriers, they restrict paracellular flux of solutes through the tight cellular junctions between epithelial cells. Therefore, solutes able to penetrate the epithelial barriers must possess either the physicochemical properties (size, charge, lipophilicity, hydrogen-bonding potential, conformation) or the structural features necessary to passively diffuse via the transcellular route or by one of the endogenous transporter systems.

Another common feature of the epithelial barriers is that they possess a low level of transcytotic activity, which restricts the permeability of macromolecules. The epithelia also act as biochemical barriers because of their ability to metabolize drugs. However, it has recently been shown that some of these epithelia (intestinal mucosa) contain apically polarized efflux systems that can restrict the passive diffusion of drugs.

If a drug successfully reaches the systemic circulation either after penetration of one of the epithelial barriers or after direct drug administration, the endothelial barriers may restrict its distribution to its site of action. From a drug delivery point of view, the most significant endothelial barriers is the BBB. Like the epithelial barriers,

the BBB serves as both a physical and a biological barrier to drug delivery. As a physical barrier, its tight cellular junctions restrict the paracellular flux of any kind of solutes. As biochemical barrier, the BBB also has metabolic capacity and apically polarized efflux systems that restrict blood-to-brain flux of certain solutes. The vascular trafficking of macromolecules is thus highly restricted and regulated.

Finally, the efficacy of drugs can be substantially reduced by the action of elimination barriers, which include the filtration system of the kidney, the MPS of the liver and spleen and the circulating leukocytes of the innate immune system. While morphologically very different, the liver and the kidney both posses mechanism to remove substances from the systemic circulation and to secrete them (or their metabolites) into excretion products such as bile and urine, respectively. The net result is a reduced blood level of the drug and thus reduced efficacy.

The immune system response to biomaterials

The administration of DDS, although constituted by biomaterials, still leads to an inflammatory response. A non-specific inflammation is the first response to an *in vivo* applied material and is immediately followed by a systemic acute response which is characterized by stress-induced activation of the innate immune system [31, 32].

The inflammation involves vascular, humoral and cellular response as it is normally promoted by microbial infection, foreign antigens (proteins, glycoproteins, carbohydrates, synthetic biomaterials) or mechanical trauma.

The mechanism involved in the defense of the body against foreign substances acts through the discrimination between self- and non-self components. This response involves the collaboration of different cell types, like polymorphonuclear leukocytes (PMNs) and monocytes/macrophages, together with the activation of the complement system, which is a mechanism implicated in the fast recognition of foreign agents, showing non-self structures into the body.

In general upon exposition to the blood, non-self substances are recognized by a process called opsonization, consisting in the adsorption of plasma proteins (opsonins) on the surface of the exogenous agent [33]. Opsonization thus targets the particles for the destructions by the phagocytic immune cells that are unable to identify directly the particles themselves. Without the opsonization process, the recognition and elimination of invading agents would be inefficient, since the macrophage would not engulf and remove them from the bloodstream.

Opsonization: the recognition of biomaterials

The opsonization process starts when the immune system recognizes a particle (bacterium, DDS, ecc.) as an intruder. The recognition stimulates the production of immunoglobulins (IgG) which are specific for the antigenic target or binding to the surface of the particle. As well components of the complement system like C3, C4, and C5 proteins are involved in the complement-mediated clearance of foreign material.

During inflammation C3, physiologically present in the blood, undergoes a hydrolysis process originating the Cb3 fragment that can bind to surface of the foreign object. The conformational change upon adsorption on a surface also triggers the Cb3 formation. Moreover the hydrolysis reaction leads to a biochemical cascade that results in the generation of also C5a fragment that contributes to label the foreign agent. The opsonization process typically takes place in the blood circulation and can take anywhere from few seconds to many days to be completed. The pattern and amount of the coating opsonins differ on the base of the physicochemical properties of the foreign material and the time of exposition.

Phagocytes carry specific surface receptors that recognize and bind C3b, as well as IgG and Ca5, and trigger a process whereby the invading particle is engulfed, surrounded and taken inside the phagocytic cell for the enzymatic digestion [34]. Phagocytes also start to release inflammatory mediators, such as histamine and proinflammatory cytokines, in order to activate and draw other phagocytes.

Although opsonization and phagocytic degradation in the bloodstream constitute the main clearance mechanisms to remove undesirable circulating components, an efficient elimination of DDS is determined by the size. The DDS that cannot be removed by the blood circulating phagocytes will be sequestered by the renal system or the liver [35], where the Kupffer cells located in the sinuses represent the largest population of macrophages in contact with the blood.

Heterogeneity of opsonization and macrophage response

The attachment of different proteins of the complement system to the DDS, known as “differential opsonization”, depends on the DDS surface charge and geometry and determines the differences in both the blood clearance and phagocyte elimination rates. According to this hypothesis, some DDS activate the complement system more efficiently and, consequently, they will be cleared faster from the blood.

For example, liposomes containing anionic phospholipids induce the activation of the complement system through the classical way, the cationic liposomes via the alternative pathway (C3b, C5a) while zwitterionic liposomes are able to activate the complement only after prolonged exposition to the blood, showing a low opsonization rate.

In the blood, the opsonins typically come into contact with exogenous components by random Brownian motion and, once close, they bind to the surface through different attractive forces including van der Waals, electrostatic, ionic and hydrophobic/hydrophilic forces [33].

Although the researchers have found some “stealth conditions” to moderate the opsonization and consequently to improve the blood circulation time and the effectiveness of the DDS, it is still impossible to avoid the carriers opsonization in a completely efficient way.

The Transendothelial migration of leukocyte in the inflammatory response

Sequential events regulate the leukocyte transmigration

Stealth DDS reach the inflamed tissues where they explicate their function. Although stealth DDS delay and weaken the innate immune response, the immune system later strengthens its action by hiring active circulating leukocytes at the inflamed site.

The response of leukocytes to any exogenous agent is characterized by their following recruitment to the inflamed site. This response encompasses a well defined multistep process consisting of: (i) leukocyte rolling adhesion, mediated by selectins, (ii) activation, triggered by chemokine signals, (iii) firm adhesion, mediated by integrins and (iv), ultimately, transendothelial migration (TEM) into the surrounding tissue (Figure 4) [36, 37]. The entire process requires about 25 min but only 1-2 min are required to pass through the endothelial cells lining the blood vessels. Although the endothelial cells constitute the primary barrier at the blood/tissue interface that leukocyte must overcome, an active interaction between the endothelial cells and the leukocytes is required to cross the vessel wall.

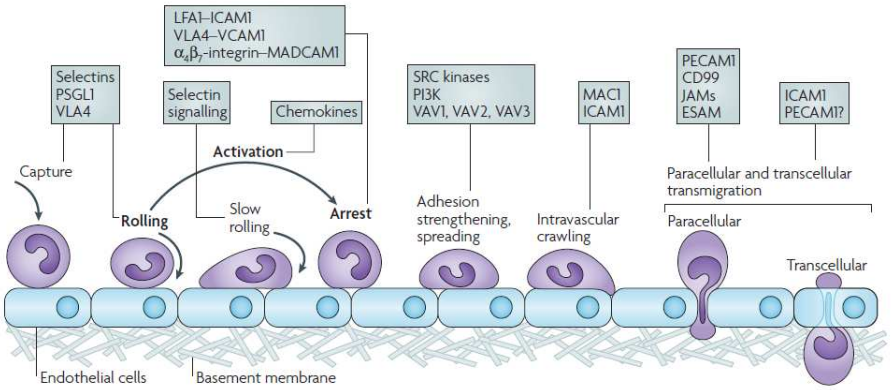

Figure 4: The three fundamental steps of the leukocyte recruitment are shown in bold: rolling, which is mediated by selectins; activation, which is mediated by chemokines, and arrest, which is mediated by integrins. However additional steps are known: capture, slow rolling, adhesion strengthening and spreading, intravascular crawling, and finally paracellular and transcellular transmigration. For each step the proteins involved in the different mechanism are shown in the boxes [38].

The importance of the endothelium in the leukocyte transmigration

The activation of the endothelium is a condition required for both the leukocyte adhesion to the vessel wall and the reaching of the inflamed tissue. At least three conditions of endothelial activation can be distinguished: immediate, that takes place in few minutes; acute, in hours; and chronic, in days. The immediate endothelium activation is driven by different chemoattractants, like the complement fragment C5a and inflammatory chemokines, and it is characterized by the endothelial contraction and intercellular gaps formation.

Nonetheless, activated endothelial cells upregulate the expression of chemokines and create both chemotactic and haptotactic gradients

essential to promote weak adhesive interactions between the circulating leukocytes and the endothelial cells [38].

Changes induced in both the endothelial cells and the leukocytes

During the step of rolling adhesion, leukocytes become loosely tethered to the blood vessel wall as consequence of their transient contact with the endothelium. The involved leukocytes weakly bind to the chemokines through their heterotrimeric G-protein-coupled receptors that immediately induce the activation of beta-2 integrin (β2-integrin), carbohydrate ligands involved in the following firm adhesion step. The β2-integrins interact specifically with selectins, adhesion molecules (inter-cellular adhesion molecules, ICAM, and vascular cell adhesion molecules, VCAM) over-expressed on the endothelial cells. The integrin-selectin interactions promote the leukocyte adhesion as well as the spreading and the intravascular crawling while preventing the detachment stimulated from the disturbing shear forces.

After interaction, the leukocytes produce cytokines, such as tumor necrosis factor-alpha (TNF-α), contribute to upregulate the expression of ICAM and VCAM on the endothelial cell surface.

The expression of ICAM and VCAM is fundamental to guarantee the following leukocyte firm adhesion. This step, indeed, is mediated by their interaction with specific leukocyte β2-integrins,such as αLβ2 (leukocyte function-associated antigen-1, LFA1; CD11a/CD18), αMβ2 (macrophage-1 antigen, Mac1; CD11b/CD18) and α4β1 (very late antigen-4, VLA4) that are over-expressed on the leukocyte membranes. The interaction induce the endothelial cell to enhance the

engagement and the clustering of both ICAM and VCAM, that are required to promote important intracellular signals that weak the cell-cell junctions, remodel the cytoskeleton, and/or induce membrane fusion events that all contribute to leukocyte TEM [39, 40].

ICAM-1. Intercellular adhesion molecule 1 (ICAM-1) is an immunoglobulin-like (Ig-like) adhesion receptor that binds the leukocyte integrin LFA-1 [41, 42]. The fundamental role of ICAM-1 in the TEM is demonstrated by the fact that the transfection of ICAM-1 alone is totally sufficient to regenerate the leukocyte transmigration across a non-endothelial cell type (CHO, epithelial) that lacks any other leukocyte adhesion receptors [43]. Moreover, Shaw and colleagues showed, by using real-time imaging, leukocytes migrating across HUVEC monolayer in which the LFA1 integrins quickly redistribute along the cell to form ring-like structures that co-cluster with ICAM1 enriched areas, localized close to the endothelial cell junctions [44].

VCAM-1. VCAM-1 mediates the adhesion of leukocytes expressing VLA-4 to the endothelium. However it is not the main player during the transmigration stage, as shown by the not significant reduction of leukocytes TEM after blocking only VCAM-1 with antibody. However blocking VCAM-1 and ICAM-1 at the same time it has an additive effect [45].

LFA-1. LFA-1 is a cell surface heterodimer of the β2-integrin subfamily. It is constituted by the non-covalent interaction of three

homologous *α* subunits (αL or CD11a) to a common β-subunit (β2 or CD18), with an extracellular inserted domain, named I-domain, that undergoes conformational changes from the closed to the open configuration for an effective ligand binding (Figure 5).

LFA-1 is the only integrin expressed on all the leukocyte lineages and acts both as a key adhesion receptor in immune and inflammatory processes and as a signal-transducing molecule [46].

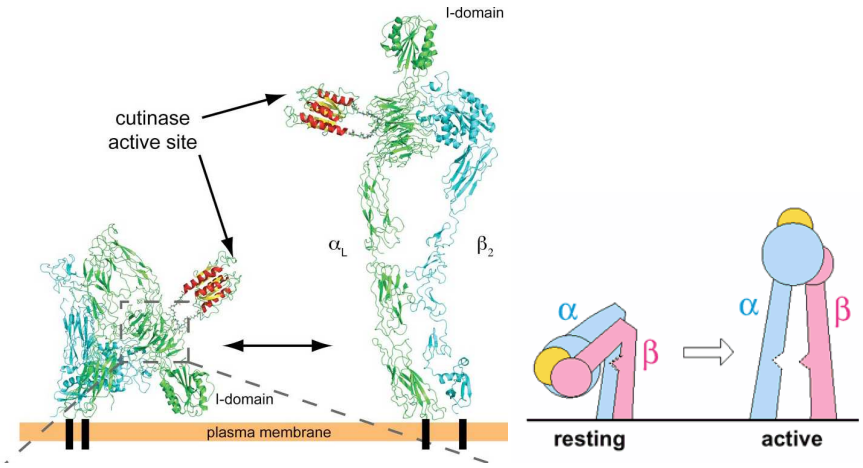

Figure 5. A. Model of LFA-1 and of bent LFA-1, composed of αL (green) and β2 (cyan) chains interacting with a fungal enzyme (cutinase) in its close (left) and opened (right) conformation. B. General model for integrin activation *(Bonasio et al, 2007)*.

Mac-1. Mac-1 is a cell surface receptor of the β2-integrin subfamily, that differs from LFA1 for the different *α* subunits (αM or CD11b) associated to the common β-subunit (β2 or CD18). It regulates the cellular adhesion by promoting the chemotaxis to end-target

chemoattractants [47]. Moreover Mac-1 is capable of recognizing and binding to many molecules found on the surfaces of invading agents.

The transendothelial route

The TEM step itself can be divided into several more discrete steps that take place before and during the actual diapedesis process. The steps before the diapedesis include the crawling in the luminal side and the production of leukocyte membrane protrusions, named pseudopodia, to sense the right stimuli and interact with the right sites on the endothelial cells. However, the endothelial cells actively participate to the leukocyte TEM through the arrangement of microvilli-like projections, named transmigratory cup structures, involved in the TEM, that finally can occur into two distinct modes: paracellular and transcellular.

The paracellular TEM demands a temporary junctional distruption while the leukocytes migrate “alongside of” or “beside” adjacent endothelial cells through pre-existing gaps at the cell borders. In contrast, transcellular TEM implies that a leukocyte transmigrates directly “through” the body of one distinct endothelial cell.

Upon crossing the endothelial cell barrier, the leukocyte must beat the underlying barrier constituted of the perivascular basement membrane, in which, anyway, there are specific regions of low matrix protein expression that are more permissive to the leukocyte transmigration [48, 49].

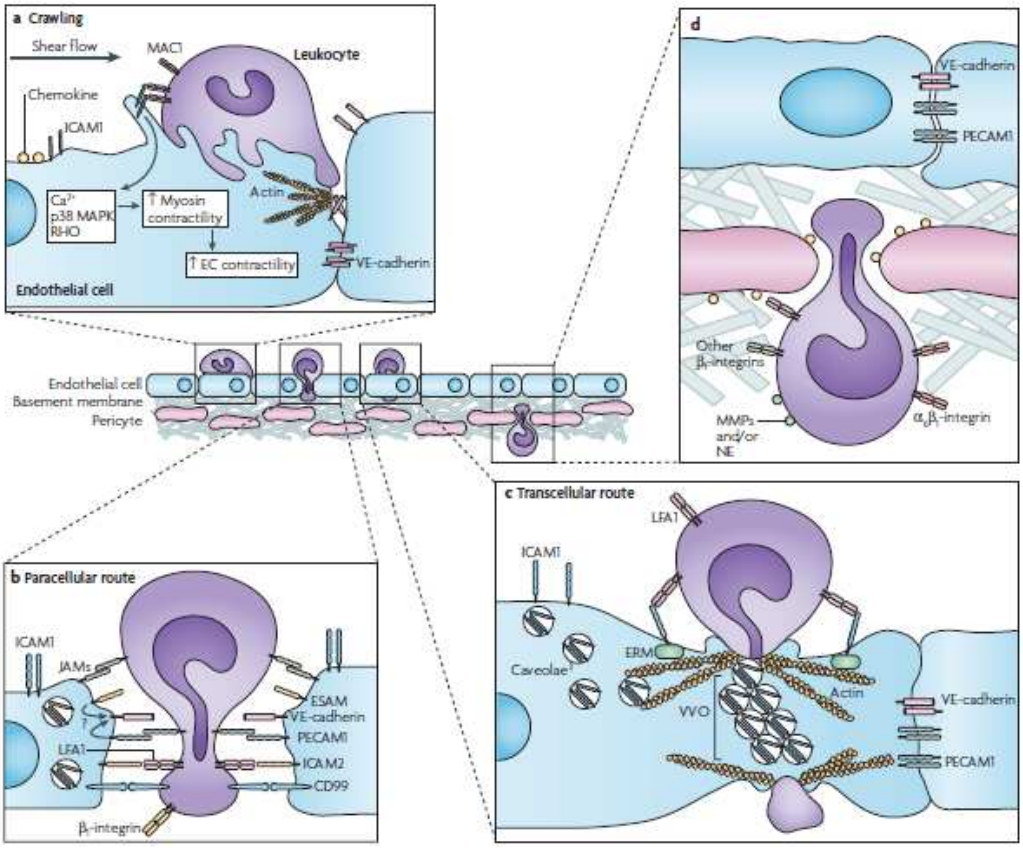

Figure 6. Migration of leukocytes through endothelial walls involves penetrating the endothelial cells and the associated basement membrane and the pericyte sheath. A. Leukocytes extend membrane protrusions into the endothelial cell while they interact with ICAM1 at the endothelial cell junctions level trough Mac-1. B. Paracellular migration involves VE-cadherin, a vascular endothelial cadherin, expressed on the endothelium, and the endothelial cell-selective adhesion molecules ICAM2. C. Transcellular migration occurs in specific parts of the endothelium in which ICAM1 ligation leads to translocation of ICAM1 to regions enriched of actin and caveolae. Caveolae enriched in ICAM1link together forming VVO that organize an intracellular channel through which a leukocyte can migrate. D. Migration across the endothelial basement membrane and the pericyte sheath is mediated by gaps between adjacent pericytes and regions of low protein deposition present in the extracellular matrix [38].

Cellular signaling events during TEM

After the leukocyte adhesion, the clustering of ICAM-1 and VCAM-1 [50] on the endothelial cell trigger the activation of different intracellular signaling pathways which induce the weakening of adhesion junctions and the remodeling of the actin cytoskeleton. These mechanisms generate the contractile forces required to induce changes in the endothelial cell shape, during the TEM. In particular the remodeling force is generated by the actomyosin contractility, produced by the activation of the Rho kinases/GTPases pathways [51].

Rho GTPase signaling. Rho activation correlates with stress fiber formation during the cytoskeletal remodeling that demand the recruitment of ERM (ezrin/ radixin/moesin) proteins to the sites of ICAM-1 clustering [52]. The ERM proteins, that usually link the cytoskeletal elements to transmembrane proteins, play an important role also in the formation of cell surface membrane structures such as microvilli and transmigratory cups particularly enriched in actin [53].

Endothelial cell apical cup structures

Additionally to the opening of intercellular junctions and the cytoskeleton remodeling, the endothelial cells actively participate to the leukocyte TEM process through the formation of endothelial microvilli-like membrane protrusions, called “docking structures”, able to attach and partially hold the adherent leukocytes [53].

According to Barreiro *et al*. these structures are enriched in ICAM-1, VCAM-1, actin, and ERM proteins [53]. The theory is that the clustering of ICAM-1 and VCAM-1 activate bound ERM proteins, on

the endothelial cell, that induce the actin remodeling and following formation of the membrane protrusions around the attached leukocyte (Figure 6).

The formation of the endothelial docking structures looks necessary in order to efficiently capture the leukocytes, especially under destabilizing shear flow conditions. However, their disassembly has to occur before the diapedesis, since they seem to act just as directional guides involved in helping the leukocytes to cross the endothelium.

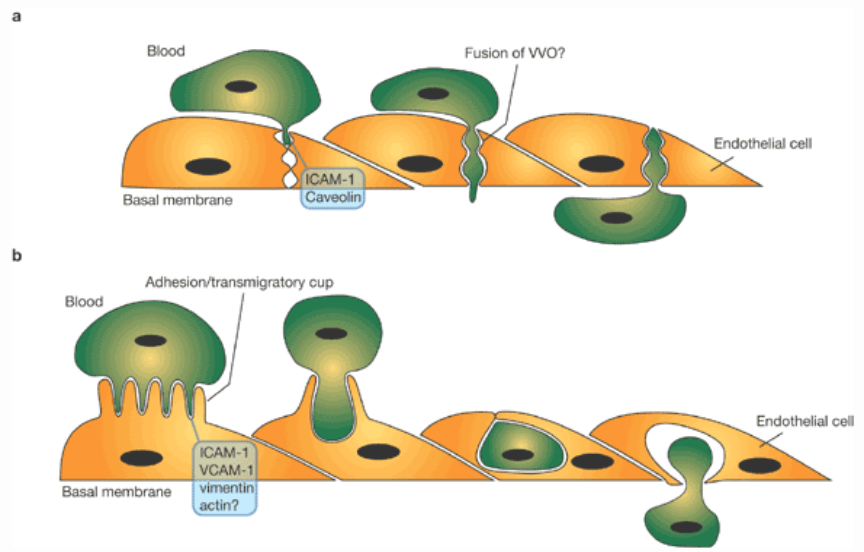

Figure 6. (a) Leukocytes can actively penetrate the endothelial cell cytoplasm by elongating pseudopods inside vesicles containing caveolin and ICAM-1. (b) When leukocytes adhere to the endothelial surface, an adhesion/transmigration cup is formed. This docking structure contains microvilli that elongate from both endothelial cells and leukocytes. The microvilli contain ICAM-1 and VCAM-1 as well as cytoskeletal proteins, such as vimentin and actin. The adhesion transmigratory cup mediates the leukocyte phagocytosis and movement towards the basal membrane of endothelial cells.

Transcellular TEM

The paracellular route is not the only route by which leukocytes extravasate. It has been shown that a relevant amount of leukocytes seemed to transmigrate through the "transcellular" route without breaching the EC junctions. They migrate directly across the cytoplasm of a single endothelial cell [54], by using a transcellular pore that accurately goes through the cytoplasm of the endothelial. Although the pores have been observed very close to the endothelial cell junctions, they are definitely distinct from them. These channels look like small circular gaps observed at the center of the ICAM1 ring-like structures, with a diameter size ranging from 0.5 to 2 µm [55]

Endothelial cell membranous structures in relation to transcellular TEM

The endothelial cells normally contain subcellular membranous structures such as caveolae, fenestrae and vesiculo vacuolar organelles (VVOs) that regulate the microvascular permeability and inflammation. These specialized membrane microdomains that have been defined as the sites that regulate the transendothelial exchange of plasma proteins in and out of the bloodstream [56], they may probably be directly or indirectly involved in the leukocyte TEM.

Although is not really clear if caveolae fuse and form VVOs and/or fenestrations, the hypothesis is that these membranous structures fuse in order to form a transcellular channel that allows the leukocyte passage. This theory is supported by the observation that lymphocytes transmigrate at areas enriched in caveolin-1, a protein caveolae-

associated [57]. It is possible that caveolae, concentrated around the transmigrating leukocyte, might fuse locally and form a transcellular pore that links the apical with the basal cell membrane. Nonetheless it's not excluded that a caveolin-independent mechanisms may exist as well, since the site of leukocyte transcellular TEM is often associated with membrane structures, apparently distinct from VVOs, that concentrate adjacent to lateral endothelial cell junctions [58]. This "endothelial cell surface-connected compartment" is constituted of membrane vesicles that upon leukocyte adhesion, continually recycle to the junctional leukocyte adhesion sites [59].

Factors regulating transcellular migration

The physiological factors that promote transcellular TEM are still not well known, since the transcellular TEM has been more easily observed *in vivo* than *in vitro,* where it looks to be the less used route. Another group observed that the intraluminal crawling of the leukocytes plays an important role in determining which route the leukocytes can take. For instance, Mac-1 deficient leukocytes usually adhere but do not crawl on the endothelial cells and they mainly use the transcellular pathway [60], after being enveloped by the endothelial cell protrusions. The formation and function of these structures is important as they help to preserve the endothelial barrier integrity while TEM is occurring [61]. A final hypothesis is that exposure to shear forces might affect transmigration route preference [62]. Thus, which factors really affect transcellular TEM is still under investigation. Another factor that can influence TEM route predilection is the endothelial ICAM-1 levels. Yang *et al*. [63]

demonstrated that transcellular TEM events were positively correlated with increased expression of ICAM-1, for example after 24 hour treatment with TNF-α. They assumed that high ICAM-1 levels influence the route of TEM since they occupy a great amount of receptors (LFA-1) on the leukocyte favoring a rapid arrest at the non-junctional sites and consequently the transcellular TEM.

Previous studies on HUVECs also demonstrated that TEM of neutrophils was exclusively paracellular on endothelial cells stimulated for only 4 hours with TNF-α, since this short-term application of TNF-α causes junctional disruption [64] However after 24 hours of TNF-α stimulation, 10% of TEM events also occurred by transcellular route [63].

Based on these observations, differences in route discrimination may depend on the strength of intercellular junctions at the inflamed site, which depends on the locally exposure to cytokines. This theory was assessed by using interleukin-1 beta (IL-1β) treatment which disrupts the endothelial cell junctions [65]. This treatment, indeed, caused a 40% decrease in the number of monocytes migrating transcellularly.

It looks like that leukocytes sense and use the path of least resistance; so if junctions are weakened, the paracellular route is preferred. It still remains to be demonstrated if an increase in transcellular TEM is observed after inhibition of the paracellular pathway by strengthening the interendothelial cell junctions. This may be a relevant explanation for the *in vivo* conditions, since the first transmigration observed was seen across vessels of the brain microvasculature, which have very elaborate and impermeable cell junctions, and it was transcellular [54].

Integrating endothelial cell membrane fusion events with leukocyte invasive podosomes

Although the endothelial cell protrusions play a main role in the leukocyte TEM, the leukocytes also contribute to this mechanism. They, indeed, extend podosome-like protrusions that sense the endothelial surface looking for a permissive location where they begin the transcellular invasion [66]. Carman *et al*. demonstrated that only the transcellular TEM is more dependent on these "invasive" podosomes, that dynamically probe to sense areas of low endothelial resistance. Once a permissive area has been recognized, the leukocyte protrusions develop into appropriate invasive podosomes which finally breach the endothelium. The leukocyte invasive podosomes interact with the endothelial transmigratory cups, which provide a vertical traction substrate approaching the endothelial cell surface [66]. Interestingly, it is often observed an abundance of vesicles or VVO-like structures in the endothelial cell cytoplasm adjacent to the invasive podosomes, which validate the idea that podosomes elicit an endothelial cell response to activate membrane fusion events that end in the formation of the transcellular pore.

Overview of leukocyte activity after transmigration

After migration in the inflamed tissue, the surrounding chemical composition of the interstitium will induce the leukocyte to phagocytose the foreign body as well as release chemokines, reactive oxygen species, growth factors, and cytokines . These released factors in turn recruit new leukocytes to the site of damage, where an aberrant

prolonged activation of the leukocytes results in an unwonted chronic inflammation.

Development of delivery strategies using smart DDS.

A multistage delivery system approach

The inability of currently used DDS to successfully negotiate the biological barriers encountered upon systemic administration greatly limits their effectiveness *in vivo* and, consequently, impacts in a significant way their translation into the clinic.

Any current therapeutic agent that exploits the possible enhanced selectivity of a DDS is not successful without an adequate strategy able simultaneously (i) to allow chemotherapeutic agent to reach the desired tumor tissue by overcoming all the biological barriers, (ii) to minimize the loss of the amount and activity and (iii) to kill selectively the tumor cells without affecting the surrounding normal cells [67].

In the last decay many progresses have been done in this orientation by also developing the idea of an innovative multistage DDS. The multistage model is based on the concept that each stage is involved in a time-sequential execution of a multi-step process: (i) the escape the immune system sequestration, (ii) the transport across the tumor endothelial wall and the interstitial space reaching the tumor mass and (iii) the release of the therapeutic agent by a controlled mechanism [68].

Recently Ferrari et al. developed a multistage delivery system constituted by a nanoporous silicon particles (NSPs) intended as first

stage vector, able to reach the tumor-associate endothelium and eventually overcome the endothelial wall, while carrying second stage nanoparticles (NP) or free drugs, which later permeate the tumor mass and explicate their primary function (Figure 7) [69].

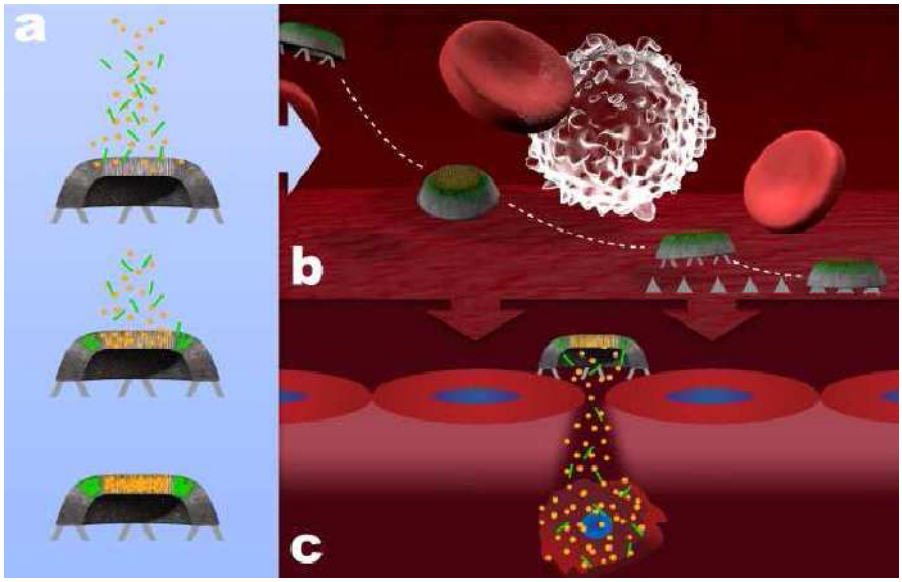

Figure 7. Schematic showing the process of the multistage DDS. (a) The first stage vector contains nanopores of specific size to load different types of second stage NP (b) The multistage DDS is superficially functionalized to travel into the blood flow, avoid RES uptake, marginate and adhere to tumor vasculature and (c) finally release the therapeutic payload .

Although silicon based materials are widely used for various biomedical applications including implantable devices, tissue engineering scaffolds due to its biodegradability, biocompatibility, the selection of silicon as material for the NSPs fabrication was also suggested by the versatility of the fabrication protocols that allow the control of shape, size and porosity [69]. Several protocols for NSPs

fabrication, indeed, have been developed by integrating top-down electrochemical porosification (etching) methods with silicon microfabrication processes. These combinations provide well-established techniques for the production and characterization of NSPs, that ensure their scalability, precision and reproducibility

In general, the fabrication of NSPs consists of two fundamental steps: the formation of the nanoporous silicon by electrochemical etching and the definition of the particles pattern by photolithography. The NSPs porous structures, indeed, depend on the combination of the electrochemical etching parameters such as the concentration of etching solution, doping, electrical current and etching time; while the geometry is precisely controlled by photolithography. By varying the process succession of porosification and lithography, a variety of non-spherical NSPs with alternative geometries, as prescribed by rational design can be fabricated (Figure 8).

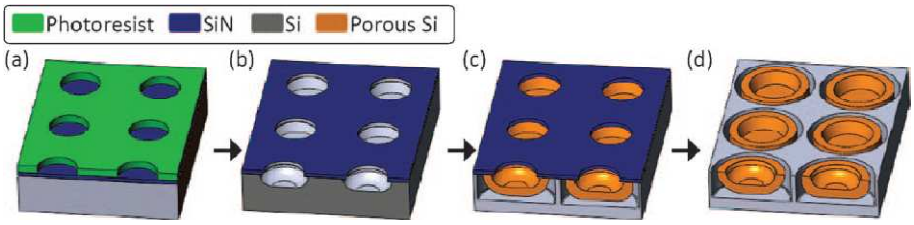

Figure 8. Schematic depiction of the NSPs fabrication process. a) Pattern transfer to the photoresist layer on top of the sacrificial silicon (SiN) layer. b) Trench formation in the silicon substrate through a combination of dry and wet etching. c) Formation of the NSPs and release layer following anodic etching. d) NSPs ready to be released by ultrasonication in isoprooanol alcohol (IPA) following stripping of the SiN mask [22].

The multistage delivery system application

The first stage NSPs, designed and engineered to carry NP, provide the first order localization at the lesion site, protect the payload from degradation and clearance and allow for its prompted and localized release. The versatile parameters for the design of NSPs make them to function as carriers for a wide spectrum of therapeutic and diagnostic free agents as well as entrapped into NP. Their loading into the porous silicon structure occurs by initial wetness method, with retention based on electrostatic interaction. Moreover the pore size and surface charge of NSPs can be adapted and properly tuned and optimized for the loading and release of different types of free molecules and NP. In general, four factors are critical to determine the loading efficiency of active agents and NP into NSPs as well as the way they will be retained and released: physic-chemical features of drugs/NP, pore size and surface potential of NSPs and, finally, conditions in which the degradation/release occur. The pore size controls the type of NP that can be loaded going from carbon nanotubes to quantum dots [69]. The loading is usually performed by the absorption method, in which the therapeutic agent is adsorbed after the DDS formation, usually by incubating the DDS with a concentrated drug solution.

The retention of the payload and its stability in circulation depend on the interaction between the payload and the carrier that is principally governed by electrostatic interactions: NSPs and NP with similar charge are indeed completely repellent. For this reason, usually the NSPs are chemically modified to change the surface charge according to the drug/NP of interest.

Additionally, the geometry of the NSPs can be optimized to efficiently penetrate into the tumor site and selectively release the payload. The particle size and shape, indeed, influence the circulation time, the flow properties and margination behavior into the vessels [70, 71] as well as its extravasation ability.

Decuzzi et al. demonstrated, via mathematical modeling, that hemispherical NSPs (Figure 9) adhere to the endothelial wall more efficiently than a spherical carrier having the same volume [71].

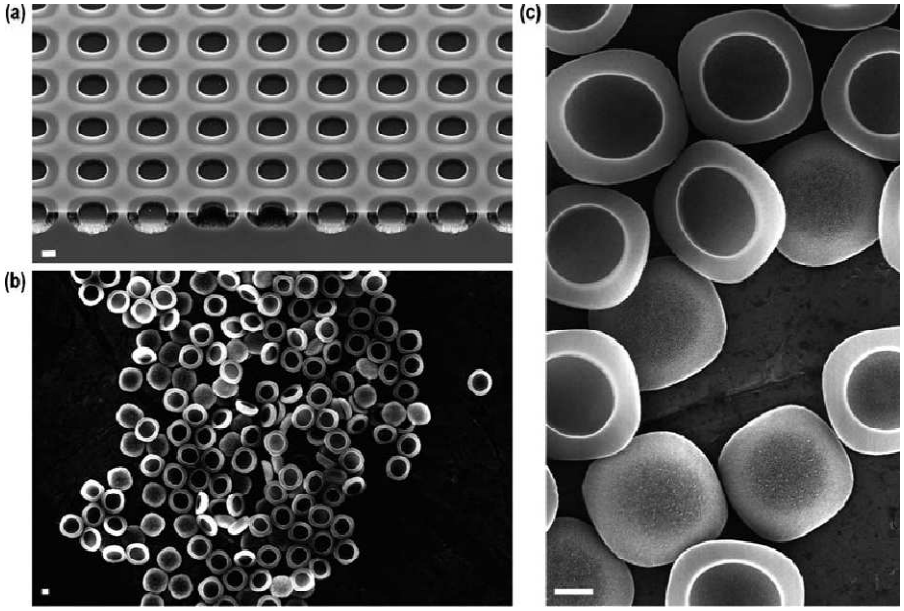

Figure 9. Scanning electron microscopy (SEM)images of large clusters of NSPs. The NSPs are characterized by size and shape uniformity. a) A etched tube-shaped NSPs still attached to the silicon substrate before the removal of the silicon nitride sacrificial layer and the NSPs subsequent release. b) Overview of a large cluster of NSPs etched bowl-shaped NSPs following release by sonication in IPA. c) Close-up of a small cluster of etched hemispherical NSPs following release by sonication in IPA [22].

Consequently, they represent the most helpful design that the first-stage vector should have to improve its margination and firm adhesion at the tumor-associated vessels [70-73], since the analogy with the flattened shape of a typical adherent leukocyte. Moreover hemispherical NSPs showed an improved cellular internalization [74, 75], that can be mediated by interaction with receptors or by caveolae, as well as a reduced cytotoxicity [76]. It has been shown that the silicon degradation product, the orthosilicic acid, is in a concentration below the daily dietary assimilation, thus the cellular proliferation, cell cycle and apoptosis processes are all unaltered [69].

Drug release from a DDS

In general, when developing a DDS it is important to consider how the used material can affect both drug release and DDS biodegradation. The release rate of the payload generally relies on: (i) drug solubility; (ii) desorption of the surface-bound or adsorbed drug; (iii) drug diffusion through the DDS matrix; (iv) DDS matrix degradation process.

The most common mechanism that controls the release of the loaded drug is diffusion. Two types of diffusion-controlled systems have been developed: the first is a reservoir device in which the bioactive agent forms a core surrounded by an inert diffusion barrier, such as liposomes; the second is a monolithic device in which the active agent is dispersed or dissolved in the inert biomaterial. As in reservoir systems, drug diffusion through and from the DDS matrix is the rate-limiting step, and release rates are determined by the material constituting the DDS and its affinity for the active agents. A weakly

bound drug is indeed rapidly released (burst release). In order to control this phenomenon DDS are coated, after drug loading, with polymers that can act as a barrier for the drug release [77].

Although the release profile is correlated to the drug loading method, the adsorption method favorites a burst release while the incorporation method guarantees a sustained release, the release from DDS is also controlled by the biodegradability rate of the materials. The rationale for using biodegradable DDS is that once the biomaterial surrounding the drug is degraded, the drug escapes. In the DDS in which the drug is covalently bound to the matrix, it is released only after bond scission by hydrolytic or enzymatic processes that take place in the local environment [78].

It has been shown that the stability of PEGylated DDS may not always be favorable for drug delivery because the DDS may be unable to easily release the active chemotherapeutic agent to after accumulation inside the tumor. In order to solve these problems, an additional function can be added to long-circulating PEGylated carriers, which allows for the detachment of PEG chains under the action of specific local stimuli that are typical of pathological areas, such as the decreased pH value or increased temperature, as noted in inflamed and neoplastic areas. In order to solve these problems, labile linkage that would degrade only in the acidic conditions of the tumor mass are well-known from the area of controlled drug release. However polymers components with pH-sensitive bonds acquire the ability to degrade and release the entrapped agents in body areas or cell compartments with lowered pH, such as tumors, inflammation zones or cell cytoplasm or endosomes. To date, a variety of liposomes have

been described that include a variety of drugs conjugates capable of releasing such drugs as adriamycin, paclitaxel, and DOX in acidic cell compartments and pathological areas.

A biomimetic strategy

A new generation of biomaterials for immune evasion

Recently, particular attention has been paid not only to the topography but also to the surface chemistry of a DDS since it is the most important parameter that influences protein adsorption, cell interaction and the host response.

The most common idea is still based on the modification of the DDS surface to minimize the long-term inflammatory effects that compromise the advantages of the DDS itself.

Currently, the alteration of the surface properties of new biomaterials have been established taking into consideration all the knowledge of the tumor biology and the immune response in order to better control the bio-responses. At the base of this idea there is the concept of "biomimetics" which consists in observing and exploring the properties of natural materials, structures and entities in order to be inspired for the realization of smart and multi-functional materials. The goal is to combine manmade with biological materials by taking advantages from the nature.

Scope of the thesis

The objective of this thesis is to demonstrate that increased localization of theranostic particles at the tumor site can be achieved by developing a novel biomimetic hybrid DDS capable of simultaneously escaping biobarriers, while targeting the cancerous lesion. In order to improve the stealth properties of the NSPs an innovative liposome formulation, composed of natural phospholipids obtained through the extraction of the cellular membranes of leukocytes isolated from the peripheral blood, has been proposed.

This new generation of liposomes composed of the same lipids and proteins of the blood circulating leukocytes are biologically inert and weakly immunogenic. Moreover the presence of some membrane proteins can transfer to the liposomes their biological functions thus improving the liposome targeting ability without requiring following surface functionalization. The leukocyte-derived liposomes can be used as coating material for the realization of biomimetic DDS called “leukolike” system (LS), since it combines the natural properties of leukocyte cells (free circulation in the blood stream, transendothelial migration and tropism towards the inflammatory site) with the characteristics of an artificial delivery system (biodegradability, biocompatibility, agents loading and release).

The LS thus demonstrates the advantages of a novel delivery strategy able to bestow a DDS with prolonged circulation, selective tumor targeting and enhanced tumor accumulation and retention.

References

1. Tao, S.L. and T.A. Desai, *Microfabricated drug delivery systems: from particles to pores.* Adv Drug Deliv Rev, 2003. **55**(3): p. 315-28.

2. Alonso, M.J., *Nanomedicines for overcoming biological barriers.* Biomed Pharmacother, 2004. **58**(3): p. 168-72.

3. Allen, T.M. and P.R. Cullis, *Drug delivery systems: entering the mainstream.* Science, 2004. **303**(5665): p. 1818-22.

4. Tyagi, R., et al., *Targeted delivery of arjunglucoside I using surface hydrophilic and hydrophobic nanocarriers to combat experimental leishmaniasis.* J Drug Target, 2005. **13**(3): p. 161-71.

5. Iyer, A.K., et al., *Exploiting the enhanced permeability and retention effect for tumor targeting.* Drug Discov Today, 2006. **11**(17-18): p. 812-8.

6. Folkman, J., *Fundamental concepts of the angiogenic process.* Curr Mol Med, 2003. **3**(7): p. 643-51.

7. Undevia, S.D., G. Gomez-Abuin, and M.J. Ratain, *Pharmacokinetic variability of anticancer agents.* Nat Rev Cancer, 2005. **5**(6): p. 447-58.

8. Hobbs, S.K., et al., *Regulation of transport pathways in tumor vessels: role of tumor type and microenvironment.* Proc Natl Acad Sci U S A, 1998. **95**(8): p. 4607-12.

9. Knop, K., et al., *Poly(ethylene glycol) in drug delivery: pros and cons as well as potential alternatives.* Angew Chem Int Ed Engl, 2010. **49**(36): p. 6288-308.

10. Gottesman, M.M., T. Fojo, and S.E. Bates, *Multidrug resistance in cancer: role of ATP-dependent transporters.* Nat Rev Cancer, 2002. **2**(1): p. 48-58.

11. Peer, D. and R. Margalit, *Fluoxetine and reversal of multidrug resistance.* Cancer Lett, 2006. **237**(2): p. 180-7.

12. Torchilin, V.P., *Recent advances with liposomes as pharmaceutical carriers.* Nat Rev Drug Discov, 2005. **4**(2): p. 145-60.

13. Reddy, L.H., *Drug delivery to tumours: recent strategies.* J Pharm Pharmacol, 2005. **57**(10): p. 1231-42.

14. Allen, T.M., *Long-circulating (sterically stabilized) liposomes for targeted drug delivery.* Trends Pharmacol Sci, 1994. **15**(7): p. 215-20.

15. Maeda, M., et al., *Sustained release of human growth hormone (hGH) from collagen film and evaluation of effect on wound healing in db/db mice.* J Control Release, 2001. **77**(3): p. 261-72.

16. Stolnik, S., et al., *Surface modification of poly(lactide-co-glycolide) nanospheres by biodegradable poly(lactide)-poly(ethylene glycol) copolymers.* Pharm Res, 1994. **11**(12): p. 1800-8.

17. Gref, R., et al., *Biodegradable long-circulating polymeric nanospheres.* Science, 1994. **263**(5153): p. 1600-3.

18. Gabizon, A.A., *Pegylated liposomal doxorubicin: metamorphosis of an old drug into a new form of chemotherapy.* Cancer Invest, 2001. **19**(4): p. 424-36.

19. Boman, N.L., et al., *Liposomal vincristine which exhibits increased drug retention and increased circulation longevity cures mice bearing P388 tumors.* Cancer Res, 1994. **54**(11): p. 2830-3.

20. Gabizon, A., et al., *Prolonged circulation time and enhanced accumulation in malignant exudates of doxorubicin encapsulated in polyethylene-glycol coated liposomes.* Cancer Res, 1994. **54**(4): p. 987-92.

21. Veronese, F.M. and G. Pasut, *PEGylation, successful approach to drug delivery.* Drug Discov Today, 2005. **10**(21): p. 1451-8.

22. Grayson, S.M. and W.T. Godbey, *The role of macromolecular architecture in passively targeted polymeric carriers for drug and gene delivery.* J Drug Target, 2008. **16**(5): p. 329-56.

23. Ferrari, M., *Frontiers in cancer nanomedicine: directing mass transport through biological barriers.* Trends Biotechnol, 2010. **28**(4): p. 181-8.

24. Muller, R.H., et al., *Phagocytic uptake and cytotoxicity of solid lipid nanoparticles (SLN) sterically stabilized with poloxamine 908 and poloxamer 407.* J Drug Target, 1996. **4**(3): p. 161-70.

25. ten Tije, A.J., et al., *Pharmacological effects of formulation vehicles : implications for cancer chemotherapy.* Clin Pharmacokinet, 2003. **42**(7): p. 665-85.

26. Katragadda, S., et al., *Role of efflux pumps and metabolising enzymes in drug delivery.* Expert Opin Drug Deliv, 2005. **2**(4): p. 683-705.

27. Bassingthwaighte, J.B., C.Y. Wang, and I.S. Chan, *Blood-tissue exchange via transport and transformation by capillary endothelial cells.* Circ Res, 1989. **65**(4): p. 997-1020.

28. Silva, G.A., *Nanotechnology approaches to crossing the blood-brain barrier and drug delivery to the CNS.* BMC Neurosci, 2008. **9 Suppl 3**: p. S4.

29. Jang, S.H., et al., *Drug delivery and transport to solid tumors.* Pharm Res, 2003. **20**(9): p. 1337-50.

30. Nies, A.T., *The role of membrane transporters in drug delivery to brain tumors.* Cancer Lett, 2007. **254**(1): p. 11-29.

31. Khansari, D.N., A.J. Murgo, and R.E. Faith, *Effects of stress on the immune system.* Immunol Today, 1990. **11**(5): p. 170-5.

32. Kushner, I., *The phenomenon of the acute phase response.* Ann N Y Acad Sci, 1982. **389**: p. 39-48.

33. Nilsson, B., et al., *Can cells and biomaterials in therapeutic medicine be shielded from innate immune recognition?* Trends in immunology, 2010. **31**(1): p. 32-38.

34. Andersson, J., et al., *Binding of C3 fragments on top of adsorbed plasma proteins during complement activation on a model biomaterial surface.* Biomaterials, 2005. **26**(13): p. 1477-85.

35. Owens, D.E., 3rd and N.A. Peppas, *Opsonization, biodistribution, and pharmacokinetics of polymeric nanoparticles.* Int J Pharm, 2006. **307**(1): p. 93-102.

36. Butcher, E.C., *Leukocyte-endothelial cell recognition: three (or more) steps to specificity and diversity.* Cell, 1991. **67**(6): p. 1033-6.

37. Springer, T.A., *Traffic signals for lymphocyte recirculation and leukocyte emigration: the multistep paradigm.* Cell, 1994. **76**(2): p. 301-14.

38. Ley, K., et al., *Getting to the site of inflammation: the leukocyte adhesion cascade updated.* Nat Rev Immunol, 2007. **7**(9): p. 678-89.

39. Cook-Mills, J.M. and T.L. Deem, *Active participation of endothelial cells in inflammation.* J Leukoc Biol, 2005. **77**(4): p. 487-95.

40. Wittchen, E.S., et al., *Trading spaces: Rap, Rac, and Rho as architects of transendothelial migration.* Curr Opin Hematol, 2005. **12**(1): p. 14-21.

41. Marlin, S.D. and T.A. Springer, *Purified intercellular adhesion molecule-1 (ICAM-1) is a ligand for lymphocyte function-associated antigen 1 (LFA-1).* Cell, 1987. **51**(5): p. 813-9.

42. Alon, R., et al., *The integrin VLA-4 supports tethering and rolling in flow on VCAM-1.* J Cell Biol, 1995. **128**(6): p. 1243-53.

43. Sans, E., E. Delachanal, and A. Duperray, *Analysis of the roles of ICAM-1 in neutrophil transmigration using a reconstituted mammalian cell expression model: implication of ICAM-1 cytoplasmic domain and Rho-dependent signaling pathway.* J Immunol, 2001. **166**(1): p. 544-51.

44. Shaw, S.K., et al., *Coordinated redistribution of leukocyte LFA-1 and endothelial cell ICAM-1 accompany neutrophil transmigration.* J Exp Med, 2004. **200**(12): p. 1571-80.

45. Ronald, J.A., et al., *Differential regulation of transendothelial migration of THP-1 cells by ICAM-1/LFA-1 and VCAM-1/VLA-4.* J Leukoc Biol, 2001. **70**(4): p. 601-9.

46. Kishimoto, T.K., et al., *The leukocyte integrins.* Adv Immunol, 1989. **46**: p. 149-82.

47. Heit, B., P. Colarusso, and P. Kubes, *Fundamentally different roles for LFA-1, Mac-1 and alpha4-integrin in neutrophil chemotaxis.* J Cell Sci, 2005. **118**(Pt 22): p. 5205-20.

48. Burns, A.R., et al., *Neutrophil transendothelial migration is independent of tight junctions and occurs preferentially at tricellular corners.* J Immunol, 1997. **159**(6): p. 2893-903.

49. Wang, S., et al., *Venular basement membranes contain specific matrix protein low expression regions that act as exit points for emigrating neutrophils.* J Exp Med, 2006. **203**(6): p. 1519-32.

50. Yang, L., et al., *Endothelial cell cortactin coordinates intercellular adhesion molecule-1 clustering and actin cytoskeleton remodeling during polymorphonuclear leukocyte adhesion and transmigration.* J Immunol, 2006. **177**(9): p. 6440-9.

51. Tiruppathi, C., et al., *Role of Ca2+ signaling in the regulation of endothelial permeability.* Vascul Pharmacol, 2002. **39**(4-5): p. 173-85.

52. Thompson, P.W., A.M. Randi, and A.J. Ridley, *Intercellular adhesion molecule (ICAM)-1, but not ICAM-2, activates RhoA and stimulates c-fos and rhoA transcription in endothelial cells.* J Immunol, 2002. **169**(2): p. 1007-13.

53. Barreiro, O., et al., *Dynamic interaction of VCAM-1 and ICAM-1 with moesin and ezrin in a novel endothelial docking structure for adherent leukocytes.* J Cell Biol, 2002. **157**(7): p. 1233-45.

54. Engelhardt, B. and H. Wolburg, *Mini-review: Transendothelial migration of leukocytes: through the front door or around the side of the house?* Eur J Immunol, 2004. **34**(11): p. 2955-63.

55. Carman, C.V. and T.A. Springer, *A transmigratory cup in leukocyte diapedesis both through individual vascular endothelial cells and between them.* J Cell Biol, 2004. **167**(2): p. 377-88.

56. Stan, R.V., *Endothelial stomatal and fenestral diaphragms in normal vessels and angiogenesis.* J Cell Mol Med, 2007. **11**(4): p. 621-43.

57. Millan, J., et al., *Lymphocyte transcellular migration occurs through recruitment of endothelial ICAM-1 to caveola- and F-actin-rich domains.* Nat Cell Biol, 2006. **8**(2): p. 113-23.

58. Mamdouh, Z., et al., *Targeted recycling of PECAM from endothelial surface-connected compartments during diapedesis.* Nature, 2003. **421**(6924): p. 748-53.

59. Mamdouh, Z., G.E. Kreitzer, and W.A. Muller, *Leukocyte transmigration requires kinesin-mediated microtubule-dependent membrane trafficking from the lateral border recycling compartment.* J Exp Med, 2008. **205**(4): p. 951-66.

60. Phillipson, M., et al., *Intraluminal crawling of neutrophils to emigration sites: a molecularly distinct process from adhesion in the recruitment cascade.* J Exp Med, 2006. **203**(12): p. 2569-75.

61. Phillipson, M., et al., *Endothelial domes encapsulate adherent neutrophils and minimize increases in vascular permeability in paracellular and transcellular emigration.* PLoS One, 2008. **3**(2): p. e1649.

62. Cinamon, G., et al., *Chemoattractant signals and beta 2 integrin occupancy at apical endothelial contacts combine with shear stress signals to promote transendothelial neutrophil migration.* J Immunol, 2004. **173**(12): p. 7282-91.

63. Yang, L., et al., *ICAM-1 regulates neutrophil adhesion and transcellular migration of TNF-alpha-activated vascular endothelium under flow.* Blood, 2005. **106**(2): p. 584-92.

64. Nwariaku, F.E., et al., *NADPH oxidase mediates vascular endothelial cadherin phosphorylation and endothelial dysfunction.* Blood, 2004. **104**(10): p. 3214-20.

65. Ferreira, A.M., et al., *Interleukin-1beta reduces transcellular monocyte diapedesis and compromises endothelial adherens junction integrity.* Microcirculation, 2005. **12**(7): p. 563-79.

66. Carman, C.V., et al., *Transcellular diapedesis is initiated by invasive podosomes.* Immunity, 2007. **26**(6): p. 784-97.

67. Cho, K., et al., *Therapeutic nanoparticles for drug delivery in cancer.* Clin Cancer Res, 2008. **14**(5): p. 1310-6.

68. Jain, R.K., *Transport of molecules, particles, and cells in solid tumors.* Annu Rev Biomed Eng, 1999. **1**: p. 241-63.

69. Tasciotti, E., et al., *Mesoporous silicon particles as a multistage delivery system for imaging and therapeutic applications.* Nat Nanotechnol, 2008. **3**(3): p. 151-7.

70. Gentile, F., et al., *The effect of shape on the margination dynamics of non-neutrally buoyant particles in two-dimensional shear flows.* J Biomech, 2008. **41**(10): p. 2312-8.

71. Decuzzi, P., et al., *A theoretical model for the margination of particles within blood vessels.* Ann Biomed Eng, 2005. **33**(2): p. 179-90.

72. Lee, S.Y., M. Ferrari, and P. Decuzzi, *Design of bio-mimetic particles with enhanced vascular interaction.* J Biomech, 2009. **42**(12): p. 1885-90.

73. Decuzzi, P. and M. Ferrari, *The adhesive strength of non-spherical particles mediated by specific interactions.* Biomaterials, 2006. **27**(30): p. 5307-14.

74. Decuzzi, P. and M. Ferrari, *The role of specific and non-specific interactions in receptor-mediated endocytosis of nanoparticles.* Biomaterials, 2007. **28**(18): p. 2915-22.

75. Decuzzi, P. and M. Ferrari, *The receptor-mediated endocytosis of nonspherical particles.* Biophys J, 2008. **94**(10): p. 3790-7.

76. Moghimi, S.M., A.C. Hunter, and J.C. Murray, *Long-circulating and target-specific nanoparticles: theory to practice.* Pharmacol Rev, 2001. **53**(2): p. 283-318.

77. Singh, R. and J.W. Lillard, Jr., *Nanoparticle-based targeted drug delivery.* Exp Mol Pathol, 2009. **86**(3): p. 215-23.

78. Heller, J., *Development of poly(ortho esters): a historical overview.* Biomaterials, 1990. **11**(9): p. 659-65.

Chapter 2

ARTICLE

Biological camouflage imparts cell-like activity to injectable particle: the leukolike delivery system

Nicoletta Quattrocchi[a,c], Ciro Chiappini[b], Massimo Masserini[c], Mauro Ferrari[a,b] and Ennio Tasciotti[a]

a) The Methodist Hospital System Research Institute, Houston, TX

b) The University of Texas at Austin, Austin, TX

c) Università degli Studi di Milano Bicocca, Monza, IT

In preparation

Keywords: leukocytes, drug delivery system, biomimetics, cancer

Abstract

Biological barriers still incapacitate therapeutic agents intravenously administered. Although several efforts have been done to improve the stealthiness of drug delivery systems (DDS), they are still unable to efficiently negotiate the phagocytic cells of the immune system and the endothelial cells of the vessels.

By taking inspiration from nature, we propose a biomimetic approach for camouflaging DDS among circulating leukocyte cells that, during inflammation are normally recruited at the lesion site via transendothelial migration (TEM).

We realized a new generation of DDS, named Leukolike system (LS), by functionalizing the surface of biocompatible nanoporous silicon particles (NSPs) with cellular membranes extracted from leukocytes. By using biological components as natural coating material the LS acquired the same surface composition and functions as those of the donor leukocyte, consequently achieving manifold advantages: a superior evasion of the immune system sequestration, an enhanced TEM while efficiently retaining and release a drug payload.

Introduction

Recent developments in biomaterials open new horizons in biomedical applications especially in the drug delivery field [1-3]. Although DDS exhibit improved pharmacokinetics and biocompatibility, several efforts are still required to develop new carriers with ameliorate performance properties: prolonged circulation time, site-specific targeting, high loading efficiency, sustained release and reduced side-effects [4, 5]. However, after intravenous injection, these biological actions are strictly affected by several DDS physicochemical factors such as size distribution, shape and surface hydrophobicity that strongly influence the interaction with plasma proteins (opsonins) and the following sequestration by the macrophages of the reticuloendothelial system (RES) [6, 7] . The activation of the immune system together with the endothelial wall represent the major biobarriers that a DDS must overcome to reach the intended target at effective concentrations [8, 9]. The DDS surface functionalization with hydrophilic elements such as polyethylene glycol (PEG) and dextrans significantly increases the blood circulation time by minimizing the opsonins adsorption to their surface [10]. The supplied hydrophilic shell makes them more invisible to the immune system and able to passively extravasate and accumulate at the tumor site via the enhanced permeation and retention (EPR) effect [6, 11] .

Based on a self/non-self discriminating mechanism, the immune response triggers an early activation of circulating leukocytes and subsequent recruitment to the lesion site, where they actively contribute to remove the invading agents [12]. The efficiency of the

immune system response strictly depends on the rapid shuttling of leukocytes from the bloodstream to the inflammatory site [13]. The leukocyte escape from the vasculature through TEM whether by the paracellular or transcellular routes [14] that involve penetrating manifold barriers: endothelial cells, pericytes and the basement membrane generated by both of these cell types [15]. TEM is predominantly mediated by the interaction between the endothelial intercellular adhesion molecule-1 (ICAM-1) and its counter-receptor lymphocyte function-associate antigen-1 (LFA-1 or CD11a) [16] that triggers the endothelial cellular contractility, required to facilitate the leukocyte diapedesis [17, 18]. However, DDS, currently used, are faraway from reproducing as naturally as possible the structures, components and properties of any blood cell and result unable to completely avoid the recognition by the immune system.

Here we realized a LS by camouflaging NSPs [19-23] trough surface coating with cellular membranes extracted from ex-vivo expanded leukocytes. We efficiently transferred both the organic and functional properties of the donor leukocytes to a manmade system, as demonstrated by biochemical and functional analysis. The biological similarity between the leukocyte and the LS surface allowed the LS to escape the macrophage phagocytosis two times more than NSPs. Additionally, in comparison to the NSPs, the LS showed an increased efficiency to retain a payload and maintain the structural integrity by avoiding the lysosomal pathway during transmigration across an endothelial monolayer. While the NSPs mostly stick and release the preloaded drug into the endothelial cells, the LS crosses the endothelial barrier and finally releases the drug in the surrounding

tumor cells, accomplishing a tumor cell killing activity twice higher than the NSPs.

The LS, therefore, represents a biomimetic DDS with unique properties that can be adapted to several types of inflammatory pathologies.

Results and discussion

Plasma membrane isolation and characterization

By taking advantage from the nature we wanted to recreate the complex properties of the leukocyte cellular membranes on the surface of the NSPs. In order to realize the LS we first attempted to isolate the plasma cellular membranes from both an immortalized line of human T lymphocyte cells (Jurkat cells) and a murine macrophage cell line (J774A.1) by ultracentrifugation in a discontinuous sucrose density gradient.

After ultracentrifugation three white lipid rings were observed at the interface between each different sucrose layer. We localized the plasma cellular membranes by screening the distribution of specific proteins associated with the different cellular membranes through immunoblotting on ten fractions collected from the top to the bottom of the gradient (Fig. 1A).

The findings showed that nucleoporin 62 (Nup62) and cytochrome c-oxidase (COX IV), a nuclear and a mitochondrial marker, localized at the supernantant-30% sucrose and at the 40-55% sucrose interfaces respectively; while CD45 and lymphocyte-specific protein tyrosine kinase (Lck), associated with non-lipid raft and lipid raft membrane regions, localized prevalently at the 30-40% sucrose interface. We

also studied the localization of the plasma membrane proteins, CD3z and LFA1 (CD11a), essential for the LS realization. CD3z is a component of the T cell receptor (TCR) that participates in the activation of T cells, while LFA1 plays a crucial role in the leukocyte TEM. Since a consistent amount of CD3z and LFA1 colocalized with the mitochondrial and nuclear membranes in the fractions # 1-3 and 9-10, we removed the membranes by centrifugation and recovered the supernatants containing CD3z and LFA1. They were pooled with the fractions containing the CD45 and Lck enriched-membrane (Fig. 1A).

Leukolike system assembly: coating of NSPs with leukocyte cellular membranes

To forge the NSPs surface close to the leukocyte's appearance, we incubated the NSPs with the isolated leukocyte membranes. In an aqueous solution the isolated membranes self-assemble into multi-bilayers lipid vesicles, ranging from the size of 200 nm to 500 nm (Fig. 1B-C), with a net negative surface charge. The surface zeta potentials was measured to be -26.44 mV, similar to the surface charge of NSPs (-28.84 mV) (Fig. 3A). We adopted a direct surface modification approach, based on silanization with aminopropyltriethoxysilane (APTES), to positively charge the NSPs surface (APTES-NSPs), whose zeta potential was measured to be 7.41 mV (Fig. 3A). When the lipid vesicles approached the APTES-NSPs reactive surface, the electrostatic interactions mediate the absorption of the lipid vesicles: once a defect occurs in the outer layer of the lipid vesicles, they fracture and spread [24] on the APTES-NSPs surface. Further spreadings led to the complete coating of the APTES-NSPs by

one or more lipid bilayers (Fig. 2C-E). Although multiple lipid bilayers can enclose the APTES-NSPs, the size was essentially unchanged (Fig. 2F).

The relevance of the APTES modification for an optimal surface coating was supported by the non-uniform coating obtained when non-modified NSPs were incubated with the leukocyte membranes (Fig. 3B). However the coating efficiency also depended by the lipid concentration of the coating solution. We prepared two diluted lipid coating solutions (1:2; 1:5) and the APTES-NSPs were partially coated, as predicted (Fig. 2C-E).

Additionally, the coating efficiency depended also by the size and lamellarity of the lipid vesicles in the coating solution: smaller vesicles with a reduced lamellarity, obtained through sonication, ensure a more uniform and smooth coating (Fig. 3Cb, Cd). However, the APTES-NSPs coated with membranes organized in larger vesicles better resembled a leukocyte (Fig. 3Cd); hence the name of LS.

Protein characterization of the LS

We next checked the protein profile of the LS surface by flow cytometry analysis, paying particular attention to the presence of CD3z and LFA1 (Fig. 3D). Under physiological conditions, CD3z is localized in the cytoplasmic leaflet of the membrane bilayer while LFA1 in the extracellular side. Because of their different membrane localizations on the leukocyte cells, LFA1 is detectable at higher levels in comparison to CD3z unless permeabilization of the cellular membrane occurs (Fig. 3D). The lower detection of CD3z and higher detection of LFA1 on the LS rather than on the uncoated NSPs

(control) suggested a correct orientation of both the proteins on the LS. However, the lower detection of both proteins on the LS in comparison to the Jurkat cells was justified by the protein loss during the membrane isolation procedure. We also confirmed the presence of CD3z and LFA1 on the LS by immunoblotting (Fig. 3E).

Ability of the LS to elude the immune system response

The feasibility of transferring some of the physical leukocyte's features to the NSPs and the strong resemblance with a leukocyte led us to verify the LS ability to escape the macrophage uptake trough a self-defense mechanism. We created two different types of LS: the first obtained by coating the NSPs with cellular membranes isolated from Jurkat cells (Jurkat-LS), and the second with membranes extracted from J774A.1 (macrophage-LS).

We seeded the J774A.1 at 30% of confluence and incubated with a population of assorted LS (ratio 1:5 cell:LS) for 3, 6 and 24 hr. Although the macrophage's innate tendency to internalize every kind of exogenous agents encountered on their way, the J774A.1 prominently phagocytosed the Jurkat-LS, whereas neglected the macrophage-LS, showing similar surface features (Fig. 4). The results obtained from a flow cytometry internalization assay showed that the uptake rate of the macrophage-LS was constant at each time point and lower than the Jurkat-LS (Fig. 4A-B). The median value observed in presence of macrophage- and Jurkat-LS was 400 and 900 respectively. In particular the highest Jurkat-LS uptake rate (median value 900) was observed after 3 hr of incubation while at 6 and 24 hr it was lower (median values 800 and 500) (Fig. 4B). The lower uptakes observed

after 3 hr were probably due to a plateau reached during the macrophage phagocytosis. In order to discriminate the two LS we previously added to the isolated Jurkat and J774A.1 membranes a distinct synthetic fluorescent lipid as a probe. The lipid nature of the probes did not alter the natural composition of the membranes (ratio 98:2 membrane lipids: synthetic lipid). In particular, the Jurkat membranes were labeled with rhodamine-phosphoethanolamine (red fluorescence), while the J774A.1 membranes with a carboxyfluorescein-phosphoethanolamine (green fluorescence).

These results were also confirmed by confocal microscopy (Fig. 4C) and scanning electron microscopy (SEM) (Fig. 4D). At the confocal microscopy J774A.1 were always seen to interact more with the Jurkat-LS and rarely with macrophage-LS, independent of the incubation time. The J774A.1 phagocytic activity was indeed clearly shown in the presence of NSPs, loaded with fluorescein isothiocyanate-bovine serum albumin conjugated to (FITC-BSA) which gives bright green fluorescence. At each time point we observed a ratio between J774A.1 and phagocytosed NSPs of 1:3 (Fig. 4C). Additionally, the SEM micrographs (Fig. 4D) showed that although the macrophage-LS were in close contact with macrophages they remained localized on the cell surface and barely totally engulfed. For the SEM analysis in which the sample needed to be a mixed population of LS we combined together only macrophages-LS and NSPs, due to optical indistiguishibility of Jurkat-LS from macrophage-LS. However all these results univocally confirmed that the J774A.1 did not recognize the macrophage-LS as an exogenous agent as much as they recognized the Jurkat-LS and the NSPs.

We then checked the non-immunogenicity of the LS as a further confirmation of its biocompatibility. We determined the levels of production of two pro-inflammatory cytokines, tumor necrosis factor-alpha (TNF-α) and IL-6, by J774A.1 in response to macrophage-LS (ratio J774A.1: macrophage-LS 1:5) after 3, 6 and 24 hr of interaction. A zymosan solution (1ng/ml) was used as positive control. We observed that zymosan induced high levels of TNF-α (450 pg/ml) immediately after 3 hr, and of IL-6 (180 pg/ml), only after 24 hr; while the macrophage-LS induce the secretion of basal levels of both TNF-α (< 100 pg/ml) and IL-6 (< 40 pg/ml) (Fig. 4E), as well as macrophages. We also showed the non-immunogenicity of NSPs and Jurkat-LS (data not shown).

Interaction of the LS with HUVEC

We investigated the LS behavior in a cellular environment by using a well established endothelial model of large vessel endothelium (HUVECs). For these experiments we seeded HUVECs at 70% confluence and treated for 24 hr with TNF-α, in order to induce an inflammatory response. After TNF-α stimulation, the media was removed and replaced with the experimental media containing the NSPs and the LS at a ratio HUVECs:NSPs/LS 1:5. The subcellular localization within the endothelial cells was detected after 3, 6 and 24 hr of incubation by transmission electron microscopy (TEM). We observed that at each time point, the LS were always surrounded by the cellular cytoplasm and maintained their integrity showing patches of coating membranes still adherent to the surface, whereas the NSPs (control) were localized into intracellular vesicles (Fig. 5A) well

defined by a lipid bilayer. Since cells usually phagocytate DDS into phagosomes, intracellular vesicles that mature in phagolysosomes by fusing with lysosome vesicles [25], we analyzed their subcellular localization with lysosomal apparatus using the RED Lysotracker lysosomal staining. The endothelial cells were treated with the RED Lysotracker solution (10ng/ml) for 1 hr by the end of each time point and immediately observed, in live, at the confocal microscope. The cells incubated with the NSPs showed a clear colocalization with lysosomes (red spots) already after 3 hr. On the other side, cells incubated with the LS (green signal associated to the coating membranes) showed no colocalization at any of all the three time points (Fig. 5B), confirming the previous TEM results. These observations indicated that the presence of the coating membranes altered the phagocytosis pathway by inducing the lysosomal escape, as leukocytes.

Intracellular retainment of the LS payload

Having observed the integrity of the LS after cellular internalization, we tested the efficiency of the LS to retain and delay the release of a payload within a cell, in comparison to the NSPs. For this purpose we preloaded NSPs with doxorubicin (DOX) before the leukocyte membranes coating. For an homogeneous coating it was required to maintain the system in continuous movement, thus causing the early release of some loaded DOX. As a consequence, the amount of loaded DOX was considered the final amount (0.061 mg) left after the coating. The same treatment was applied to the non-coated NSPs (0.059 mg).

The release study was conducted leaving both the NSPs and the LS at 37°C, in continuous movement. We checked the release after 30 min, 1 and 1.5 hr (burst release) as well as after 1, 2 and 3 days (sustained release) (Fig. 6A). At each time point the samples were centrifuged at 500 rpm, the surnatants were saved and the pellets resuspended into 250 µl of fresh phosphate buffered saline (PBS), pH 7.2. The drug concentration was estimated as a linear function of the absorbance, read at 480 nm, as determined by the standard curve.

The DOX burst release from the two systems was really different: after 1.5 hr, 80% of loaded DOX was already released from the NSPs, while only the 20% from the LS. Consequently, after 2 days, when the NSPs totally released the loaded DOX, the LS released only the 40% of the payload, suggesting a retaining function of the coating membranes (Fig. 6A). The release profile did not change by changing the loaded agent. We repeated the experiments using FITC-BSA as payload (Fig. 6B). In this case a prolonged retainment of FITC-BSA from the LS was observed until the second day while after 1 day the NSPs released 100% of the loaded FITC-BSA (Fig. 6B).

On the basis of these results, the LS retaining property was also checked in a cellular system. We incubated the NSPs (control) and the LS, both carrying FITC-BSA (Fig. 6C), with TNF-α activated HUVECs (70% confluence), in a HUVECs:NSPs/LS ratio of 1:5. The coating membranes were labeled with the synthetic red fluorescent lipid for tracking their intracellular fate. The release was checked after 2 hr, 1 and 2 days looking for the FITC-BSA fluorescent signal at the confocal microscope. The expected green fluorescence intensity in the area surrounding the particles was observed only after 24 hr within the

cells carrying the NSPs. At the same time point no significant green fluorescent signal was observed around the LS, even thought a diffuse red fluorescence intensity was observed into the cytoplasm. After 48 hr the green fluorescent signal was stronger and more spread all around the NSPs. An increased green fluorescence intensity was also seen in the area surrounding the LS, where the red fluorescent signal became stronger too (Fig. 6D). The observed results confirmed the theory of the preserved integrity of the LS for 24 hr that justifies the delayed release of the payload, both within and without the cells, by comparison with the NSPs.

Transmigration ability of the LS

Thinking at the LS as a device able to mimic the leukocyte properties, we verified its ability to transmigrate through the endothelial monolayer, like real leukocytes, while delivering a therapeutic agent.

We examined the transmigration ability using 24-well transwell inserts constituted by a polycarbonate microporous membrane with a 8 µm pore size. We seeded HUVECs (about 4x10^5) on the upper side of the transwell membrane and let them adhere and spread until 100% confluence. We established the best condition to obtain a confluent HUVECs monolayer after seeding HUVECs at different dilutions and checking the confluence with crystal violet staining. When the monolayer reached 100% confluence, the media in the upper chamber was replaced with experimental media containing DOX loaded NSPs or LS in a concentration that respected the ratio 1:5 cell:particles. The cells were incubated for 24 hr allowing the particles to transmigrate toward the underside of the transwell insert. The

number of NSPs and LS that migrated to the bottom surface of the wells was determined by acquiring at the optical/fluorescent microscope four non-overlapping random fields on each well. The experiments were repeated in triplicate. The particle number of each field was estimated using ImageJ software and the averages reported in the graph (data not shown). The results showed that the transmigration ability of the LS was higher than the NSPs one.

As a following step we tested the tumor killing ability of the LS on breast cancer cells (MDA-MD-231) seeded at the bottom of the lower chamber of the transwell system. After crossing the endothelial monolayer the LS interact with the MDA-MD-231 cells while releasing the DOX payload (0.39 mg). The DOX-associated cytotoxic effect was evaluated by MTT assay and we observed that the cell viability decreased rapidly in presence of LS in comparison to NSPs as a dose-dependent result. MDA-MD-231 treated with and without free-DOX were used as controls (data not shown).

Discussion

In biomedical research the most important concern raised related to the way of controlling the physical-chemical properties of materials for obtaining a specific biological behavior [26]. In order to achieve this aim, researchers started to investigate the surface features of the body's own cells, such as the blood cells.

We proposed the LS as a feasible example of a synergic combination between artificiality and nature. To our knowledge the LS represents the first successful attempt to realize an innovative DDS that integrates the features of an artificial delivery system

(biodegradability, biocompatibility, agent loading and release) with the natural properties of the leukocytes (free circulation in the blood stream, TEM and tropism towards the inflammatory site). By combining together all these properties we aimed to create a hybrid system able to reach the intended site successfully and to release a theranostic agent at an effective concentration.

So far we demonstrated that the leukocyte cellular membranes can be used as a natural coating material, ideal to confer on artificial device some of the properties of a blood cell. A part from showing the same protein/lipid composition, the LS also resembled the figure of a leukocyte, minimizing its recognition from the immune system. By evading from the macrophage uptake, the circulation time increases, offering to the LS a higher chance to reach the interested site. The LS thus looks more promising than others DDS that, on equal circulation time, require different chemical surface modifications that make them more visible to the immune system.

Moreover our hybrid system showed the ability to overcome the endothelial cells lining a vessel wall. During the TEM, the LS escapes the lysosome pathway, at which any exogenous agent is commonly destined, preventing the enzymatic degradation of the coating membranes and a burst release of DOX at the endothelial level. We believed that the intracellular interaction between LFA1, exposed on the LS surface, and ICAM1, expressed in the stimulated HUVECs, activated the signaling pathways involved in the endothelial cytoskeletal remodeling and contractility during the leukocyte diapedesis [27]. The active interaction between the proteins on the LS surface and the endothelial cells during the transmigration was

confirmed by the lower transmigration rate of the NSPs. Probably NSPs could transmigrate only through the paracellular route and not by the intracellular pathway that is mediated by LFA1/ICAM1 interaction. Additionally, the NSPs entrapped into the lysosomal vesicles were probably degraded or eventually released very late.

The LS thus showed some of a leukocyte properties increasing the possibility to reach the inflammatory site and release the payload in response to the environmental conditions. The acidic pH of the tumor matrix and the secreted enzymes will lead to the coating membrane dissolution and the consequent DOX leaking and uptake by tumor cells. The LS can be also internalized by the tumor cells and release the therapeutic agent directly into their cytoplasm.

In conclusion, all these properties suggested a possible biomedical application of the LS as optimal DDS.

In the cancer therapy, however, a specific targeting strategy is required. Before feature testing on animal models, the targeting ability of the LS will be improved by using cellular membranes of primary leukocytes *ex-vivo* expanded and genetically modified. The possibility to improve the leukocyte tumor tropism by genetically inducing the expression of specific tumor targeting agents offers an additional tool to optimize the LS and to apply to different cancer types as well as to all the vast array of pathologies which involve inflammation.

Material and Methods

Cell cultures

The immortalized T lymphocytes cell line (Jurkat), the murine macrophage cell line (J774A.1), the human umbilical vein endothelial cell line (HUVEC) and the human breast cancer cell line (MDA-MB-231) were all purchased from the American Type Cell Collection (ATCC). Jurkat cell suspensions were grown in RPMI-1640 medium (GIBCO) supplemented with 10% fetal bovine serum (FBS), 1% glutamine and 1% antibiotic antimycotic solution (Pen-Strep). J774A.1 and MDA-MB-231 cells were cultured in α-minimum essential medium (α-MEM) supplemented with 10% FBS and 1% Pen-Strep. HUVEC were cultured in recommended EGM-2-MV medium supplemented with EGM-2-MV singlequots and 5% FBS. The cells were kept in a humidified atmosphere, at 37 °C, containing 5% CO_2.

Plasma membrane isolation

$2.8x10^8$ cells were centrifuged at 500 g for 10 min at 4 °C and the pellet resuspended in 2 mL of complete homogenization buffer (HB) (25mM sucrose, 10mM Tris/HCl, 1mM $MgCl_2$, 1mM KCl, 2mM phenylmethylsulfonyl fluoride (PMSF), trypsin-chymotrypsin inhibitor 200 ug/mL, DNase 10 ug/ml, RNase 10 ug/ml final concentration; Sigma-Aldrich) pH7.3. Cells were enucleated in a hand-held Dounce homogenizer (20-30 passes in ice) and centrifuged at 500 g for 10 min at 4 °C. The supernatant was collected and the pellet resuspended in HB. The homogenization and centrifugation

steps were repeated until the pellet was free of intact cells, checked by light microscopy. The supernatants were pooled and lied on a discontinuous sucrose density gradient composed of 55% (w/v), 40% (w/v), 30% (w/v) sucrose in a 0.9% normal saline solution (NSS). The discontinuous gradients were ultracentrifuged in a Beckman SW-28 rotor at 28.000 g for 30 min at 4 °C, using polycarbonate tubes. The plasma membrane-rich region was collected at the 30/40% interface. Ten fractions were collected from the top to the bottom of the gradient for successive protein characterizations. The plasma membrane-rich region was diluted two-fold with NSS and ultracentrifuged in a Beckman SW-28 rotor at 28.000 g for 1h at 4 °C. The pellet was resuspended in two-fold NSS and ultracentrifuged again at the same conditions. The isolated membranes were lyophilized over night, weighted and stored at 4 °C after rehydratation in a minimal amount of NSS.

Immunoblotting

The distribution along the gradient of proteins associated to nuclear, mitochondrial and plasma membranes was analyzed by dot-blot procedure. Briefly, 2.5 µl of each fraction were spotted on a polyvinylidene fluoride (PVDF) membrane . The membrane was blocked with 5% milk, 0.1% Tween-20 in PBS solution, followed by sequential incubation with primary antibody (1:5000 dilution) and HRP-conjugated mouse anti-human IgG secondary antibody (1:10000 dilution) (SantCruz Biotechnology). The blots were developed using SuperSignal West Dura chemiluminescent substrate (Pierce) and the luminescent signals recorded on X-ray film using a Konica SRX-

101A X-ray processor. The monoclonal antibodies (mAb) used as primary Ab were: anti nucleoporin p62 (np62), COX IV, Lck, CD45, CD3z (SantaCruz Biotecnology) and LFA1 (CD11a) (Biolegend).

LS assembly

The protein concentration of the isolated plasma membranes was quantified by Bradford assay (BioRad). The lipid concentration was estimated considering the protein to lipid ratio 1:1 by weight. The membrane solutions were always diluted in a such way to have a final lipid concentration of 1 mg/ml.

NSPs ($1.5x10^6$) with a diameter of 2.8 µm, oxidized or superficially modified with APTES, were incubated with the lipid membrane solution over night, at 4°C under continuous rotation. In some conditions the membrane solution was sonicated for 45min at 45°C before incubation with the NSPs. Lipid membrane solutions with a dilution factor of 1:2 and 1:5 were also prepared.

After incubation, the not-bonded membranes were washed away from the membrane coated NSPs (LS) by centrifugation at 500 rpm for 10 min at 4°C. The same conditions were applied for all the LS realized (*Jurkat-LS* and *macrophage-LS* were realized using membranes isolated from Jurkat and J774A.1 cells respectively).

Fluorescent LS were realized for flow cytometry and confocal microscope analysis. A synthetic fluorescent lipid (1,2-dioleoyl-sn-glycero-3-phosphoethanolamine-N-carboxyfluorescein (PE-FITC) or 1,2-dioleoyl-sn-glycero-3-phosphoethanolamine-N-lissamine-rhodamine-B-sulfonyl (PE-Rhod)) was resuspended into the lipid

membrane solution, with a final lipid molar ratio 2:98. The molecular weight of the phosphatidylcholine was considered as the mean molecular weight value of the isolated membranes.

The ζ-potential measurements of NSPs, LS, lipid membrane solutions and Jurkat cells were performed in phosphate buffer (pH 7) using a Zeta PALS Zeta Potential Analyzer (Brookhaven Instruments Corporation; Holtsville, NY). The average sizes were determined at the Multisizer™ 4 Coulter Counter (Beckman Coulter).

Transmission electron microscopy

The samples were fixed with a solution containing 3% glutaraldehyde (GTA) and 2% paraformaldehyde (PFA) in 0.1 M cacodylate buffer, pH 7.3. After fixation, the samples were washed and treated with 0.1% Millipore-filtered cacodylate buffered tannic acid, postfixed with 1% buffered osmium tetroxide for 1 h, and stained en bloc with 1% Millipore-filtered uranyl acetate. The samples were dehydrated in increasing concentrations of ethanol, infiltrated, and embedded in Spurr's low viscosity medium. The samples were polymerized in a 70°C oven for 2 days. Ultrathin sections were cut in a Leica Ultracut microtome (Leica, Deerfield, IL) stained with uranyl acetate and lead citrate in a Leica EM stainer, and examined in a JEM 1010 transmission electron microscope (JEOL, USA, Inc., Peabody, MA) at an accelerating voltage of 80 kV. Digital images were obtained using AMT Imaging System (Advanced Microscopy Techniques Corp, Danvers, MA).

Scanning electron microscopy

Samples were spotted onto a metal stub, dried inside a vacuum desiccators over night and coated with a thin layer of gold (5 nm) using an SEM gold sputter before the acquisition of digital images using a FEI quanta 400 ESEM FEG instrument equipped with an ETD (SE) detector or a Hitachi S-5500 SEM apparatus.

Flow cytometry

Surface staining of Jurkat cells (1x10^6), NSPs (2x10^5) and LS (2x10^5) were performed in ice cold PBS 1x, 10% FBS, 1% sodium azide. Primary labeled antibodies, FITC-conjugated anti-CD3z mAb or/and APC-conjugated anti-CD11a mAb, were added and incubated for 1h at 4°C in the dark under continuous rotation. For the intracellular staining of the CD3z domain, Jurkat cells were previously permeabilized in 0.01% Tween-20 for 4 min. Opportune isotypes of the IgG FITC- and APC-conjugated mAb were used as negative control at the same conditions. After washing, the samples were then analyzed with a Becton Dickinson FACS Calibur equipped with a CellQuest software. Five thousand events were evaluated for each experiment. The results are the average of three experiments.

Macrophage uptake of the LS

J774A.1 cells were seeded at 30 % confluence and incubated with: APTES-NSPs alone (control), Jurkat-LS alone (positive control), macrophage-LS alone (negative control), a mixed population containing NSPs and macrophage-LS (for SEM analysis), Jurkat- and

macrophage-LS labeled with PE-Rhod and PE-FITC respectively (for confocal microscopy and flow cytometry); with a ratio cell:particles 1:5. The samples were analyzed after 3, 6 and 24 hr incubation by SEM, confocal microscopy and flow cytometry.

For SEM analysis samples were fixed using a solution containing 2.5% GTA. After fixation, the samples were washed and dehydrated using 30, 50, 70, 90, 95 and 100% ethanol serial dilution steps, followed by dehydratation in 50 % ethanol-hexamethyldisilazane (HMDS) and pure HMDS solution. Samples were dried for 2 days in a desiccator before sputter coating with 5 nm layer of gold and observation by using a FEI quanta 400 ESEM FEG instrument.

For the confocal microscopy analysis, the J774A.1 cells, seeded in 4 chambers glass slides, were fixed in 4% PFA solution for 20 min, washed two times with PBS, permeabilized using 0.1% Triton-X 100 solution for 4 min and washed with PBS two times. After 30 min incubation with 1% bovine serum albumin (BSA) blocking solution, the cellular cytoskeleton staining was performed with Alexa-Fluor 594-Phalloidin (Invitrogen) for 30 min, followed by the nuclear staining with DRAQ5 (Biostatus Ltd) for 45 min. All the steps were completed at room temperature (RT), by preventing light exposure. After staining, the chambers were removed, a drop of ProLong Gold mounting medium was added and the coverslip mounted on. The samples were observed using a Leica DM6000 upright confocal microscope equipped with a 63× oil-immersion objective.

A flow cytometry analysis was accomplished to quantify the percentage of PE-FITC and PE-Rhod positive cells as a measure of macrophage uptake. The J774 cells were detached from the wells by

gentle scraping with a cell scraper, fixed with 4% PFA and analyzed with a Becton Dickinson FACS Calibur equipped with a 488-nm Argon laser and CellQuest software.

Cytokines analysis

J774A.1 macrophages were cultured overnight in 24-well plates at a 30% confluence containing 1 mL medium. After 24 hr the cells were incubated with fresh medium (600 μl) containing NSPs, macrophage-LS, Jurkat-LS and macrophage-/Jurkat-LS (1:5 cell:particles). Zymosan at 10 ng/mL concentration (Sigma, USA) was used as a positive control for cytokines production and untreated cells were used as a measure of basal levels of cytokine release. The cell culture supernatant was collected at 3, 6, and 24 hr and stored at –80 °C. Samples were analyzed according to the manufacturer's instructions using a Abcam mouse-TNF-α and mouse IL6 cytokine kit ELISA (Abcam). Cytokine levels were read on a SPECTRA max M2 plate reader (Molecular Devices). The quantification was carried out based on standard curves for each cytokine in the concentration range of 1–1000 and 1-500 pg/ml respectively.

LS interaction with endothelial cells and subcellular localization

HUVECs were grown until 70% confluence and stimulated with tumor necrosis factor alpha (TNF-α) 10 ng/mL, for 4 h at 37 °C. After activation HUVECs were incubated with APTES-NSPs (control) and LS labeled with PE-FITC (ratio cell:particles 1:5) for 3, 6 and 24 h at 37 °C. Samples were prepared for TEM analysis as previously

described. In some experiments cells were incubated for 1 h by the end of the incubation time with a Red LysoTracker solution 10 ng/ml for the lysosomal staining. The LysoTracker solution was washed away with PBS-glucose buffer (GIBCO). Live images were acquired within 1 h using a Leica DM6000 upright confocal microscope equipped with a 63× oil-immersion objective.

LS loading and release profile of a payload

APTES-NSPs (1×10^8, 2.8 µm) were resuspended into 200 µl of a FITC-BSA solution (5mg/ml) for 2 h at 4°C in the dark, under continuous rotation. Samples were then centrifuged at 2000 rpm (Beckman Coulter Allegra X-22 Centrifuge equipped with a 296/06 rotor) for 5 min to remove the free unloaded FITC-BSA. The amount of FITC-BSA in the supernatant was quantified evaluating its emission peak at 488 nm using a UV-vis spectrophotometer. The fluorescence was converted into a concentration (µg/mL) of BSA using a standard curves obtained at known FITC-BSA concentrations. The FITC-BSA loaded NSPs were mixed with 200µL of 1 mg/ml coating membrane solution and incubated at 4°C for 2h under continuous rotation. FITC-BSA loaded NSPs used as control were subjected to the same procedure. Samples were then centrifuged at 1000 rpm for 5 min to remove the no-bonded membranes and the amount of FIT-CBSA released during the coating step. The amount of loaded FITC-BSA left into the NSPs and the LS was then estimated.

The release profile of FITC-BSA from NSPs and LS was evaluated maintaining the systems in a moving condition. The supernatant was taken out at established time (30 min, 1hr, 1.5hr, 24hr, 48hr, 72hr) and

replaced with 200 μL fresh NSS. The fluorescence of FITC-BSA at 488 nm was reported and the cumulative release of FITC-BSA was calculated. Statistical analysis of the release from the two different systems (NSPs/LS) were conducted. ANOVA analysis was carried out, and $\alpha = 0.05$ used as significant level.

The same procedures were applied for determining the loading and release profile of DOX. The DOX solution had a concentration of 2 mg/ml and the absorbance peak was at 490 nm.

Intracellular LS release profile of a payload

HUVECs were seeded, grown until 70 % confluence and stimulated with TNF-α at the conditions already described. HUVECs were incubated with FITC-BSA NSPs (control) and FITC-BSA LS. In these experiments the LS was realized using PE-Rhod enriched lipid membranes. After 2, 24 and 48 hr of incubation, the cells were fixed with 4% PFA solution and prepared for confocal microscopy analysis applying the staining protocol described above. The images were acquired using a Leica DM6000 upright confocal microscope equipped with a 63× oil-immersion objective.

LS transmigration ability

24-well transwell inserts constituted by a polycarbonate microporous membrane with a 8 μm pore size were used. HUVECs (about 2x10^5) were seeded on the upper side of the transwell membrane and let them adhere and spread until a 100% confluence. The confluence was checked with crystal violet staining. 200 μl of media in the upper chamber was replaced with 200 μl of experimental media containing

NSPs and LS (cell:particles ratio 1:5). In the lower chamber 600 µl of PBS were added in order to avoid that experimental media went through the membrane. After 24 hr, the number of loaded NSPs and LS that migrated was determined by acquiring at the microscope four nonoverlapping random fields on each well, and three wells were analyzed for each experimental point. The number of transmigrated NSPs and LS was estimated by ImageJ software.

MTT cell proliferation assay

MDA-MB-231 cells were seeded in 24-well plates at 50000 cells well in EGM-2-MV media enriched with TNF-α 10 ng/ml, in a final volume of 600 µl, and transwell inserts prepared as previously described were introduced into the well. 24 hr later the media into the transwell insert was removed and substituted with 200 µl of fresh media containing NSPs and LS both preloaded with DOX, at a ratio 1:5 cell:particles. At 24, 48, 72 and 96 hr, the medium was removed and medium containing 0.5 mg/mL of 3-(4,5-dimethylthiazol-2-yl)-2,5-diphenyltetrazolium bromide(MTT, Sigma-Aldrich) was added at 200 µl well for 4 h at 37 °C to the appropriate plates. Medium was then removed and 200 µl of dimethylsulfoxide (DMSO, Sigma-Aldrich) was added to each well. After 30 min at RT, the absorbance was read at 570 nm using a SPECTRA max M2 plate reader (Molecular Devices).

Figure legends

Figure 1. A. Membrane isolation through a discontinuous sucrose density gradient and immunoblotting of specific cellular membrane markers along the gradient fractions. In the white boxes are indicated the fractions containing the plasma cellular membranes enriched in the interested proteins LFA1 and CD3z. The cellular lysate was used As positive control, the 55% sucrose solution as negative control. B. Transmission electron micrograph (TEM) of leukocyte isolated membranes organized into lipid vesicles. C. Particular of B showing the lipid bilayer structure of a singular vesicle.

Figure 2. A-E. TEM and scanning electron microscopy (SEM) micrographs showing the adsorption of isolated leukocyte membranes on NSPs. The coating efficiency depends on the lipid concentration 1:5 (C), 1:2 (D), 1 (E) of the membrane solutions. In TEM are shown both the coronal and transversal sections of the bare NSPs (B) and LS (C-E). The SEM micrographs show how the porous surface of NSPs looks before and after coating with membrane solutions containing a different lipid concentration. The different coating efficiencies are clearly visible in the corresponding magnifications, on the right. F. The size distribution of the NSPs diameter does not change after membrane coating as shown in the graph.

Figure 3. A. Net surface charge (zeta potential) reading for the isolated membranes, NSPs before and after APTES surface functionalization, LS and Jurkat cells. B. SEM micrographs of the LS (b and d) realized using oxidized- (a) or APTES-modified NSPs (c).

The images show how the different surface net charge of the NSPs surface plays an important role in the interaction with the isolated membranes. C. 3D reconstitution of NSPs (a) and SEM micrographs of LS made with different coating procedures (sonication (b), no-sonication (c)) and of a real leukocyte. D-E. Flow cytometry analysis and immunoblotting showing the protein (CD3z, LFA1) composition of the LS surface (histograms on the right) in comparison with the Jurkat cells (histograms on the left).

Figure 4. A-B. Flow cytometry analysis and corresponding histograms of macrophage-LS (green) and Jurkat-LS (red) uptake rate in presence of J774A.1. C. Confocal microscopy of macrophage-LS (green) and Jurkat-LS (red) (upper row), and NSPs (lower row) uptake rate in presence of J774A.1 after 3, 6 and 24 hr of incubation. In the lower row NSPs were labeled by loading bovine serum albumin conjugated to fluorescein isothiocyanate (FITC-BSA) (green) D. SEM micrographs of Jurkat-LS (upper row) and macrophage-LS (lower row) uptake rate in presence of J774A.1 at 3, 6 and 24 hr respectively. D. Pro-inflammatory cytokines (TNF-α, IL-6) production by murine macrophages treated with zymosan suspension of 1ng/ml and macrophage-LS for 3, 6 and 24 hr. TNF-α and IL-6 levels were assayed by ELISA. Data are representative of 3 experiments.

Figure 5. A. TEM micrographs and (B) confocal images showing NSPs colocalization with lysosomes (left column) and LS localization into the cytoplasm (right column) after internalization by HUVECs at 2h (upper panels), 4h (middle panels), 24h (lower panels). In the confocal images lysosomes were stained with Lysotracker Red (1 uM)

for 1h, NSPs are shown trough bright field while the LS is labeled with green fluorescent lipids. A magnification of each boxed region is shown at the corner of the correspondent panel.

Figure 6. A-B. DOX- and BSA-release profile from NSPs (red) and LS (green). The release profiles have been checked in PBS pH 7.4 in moving condition for few days. A burst release at 0.5, 1 and 1.5 hr is shown in the inserts. All the experiments were done in triplicate. C. Confocal microscopy images of LS loaded with FITC-BSA (a) and coated with leukocyte membranes stained with a rhodamine-lipid (b). The correspondent merge and bright field are shown in the panels c and d. D. Confocal microscopy images of FITC-BSA (green) release from NSPs and LS (described in A) after 2, 24 and 48hr of internalization with HUVECs. The FITC-BSA release starts at 24hr prevalently from NSPs and it is more evident after 48hr, as seen in the upper panels showing only the channel of the FITC-BSA. Some FITC-BSA from LS can be poorly observed after 48hr. At 24hr the coating membranes start to dissociate from the LS as shown by the spreading of the red fluorescence in the lower panels.

Figure 1

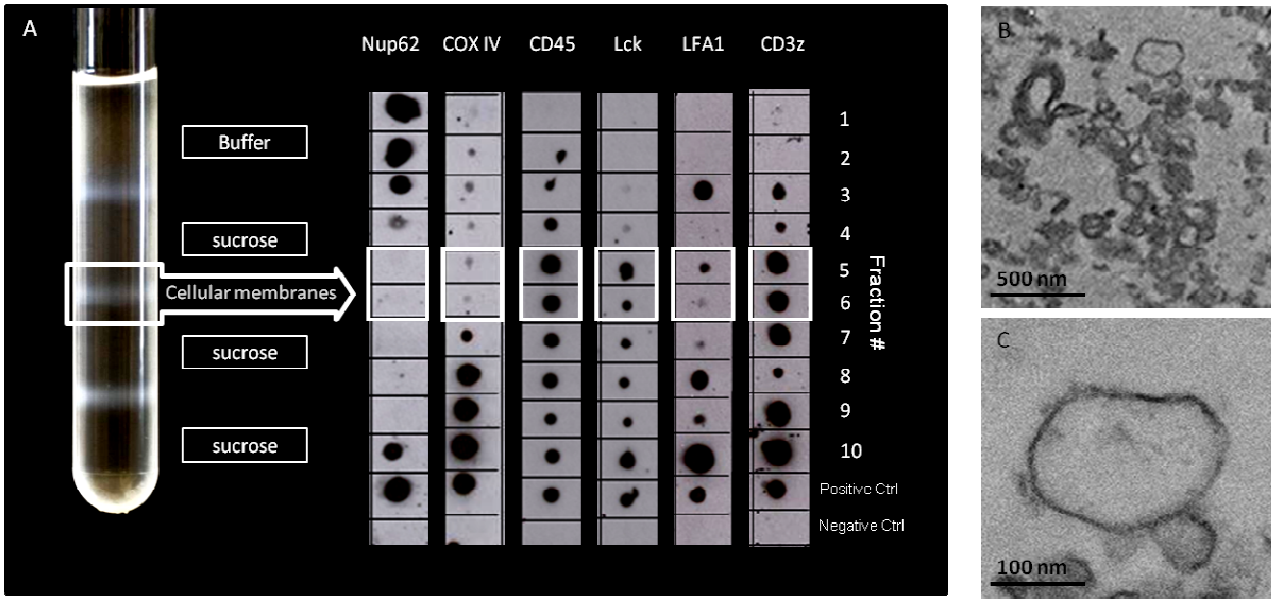
A
Nup62
COX IV
CD45
Lck
LFA1
CD3z
Buffer
sucrose
Cellular membranes
sucrose
sucrose
1
2
3
4
5
6
7
8
9
10
Fraction #
Positive Ctrl
Negative Ctrl
B
500 nm
C
100 nm

Figure 2

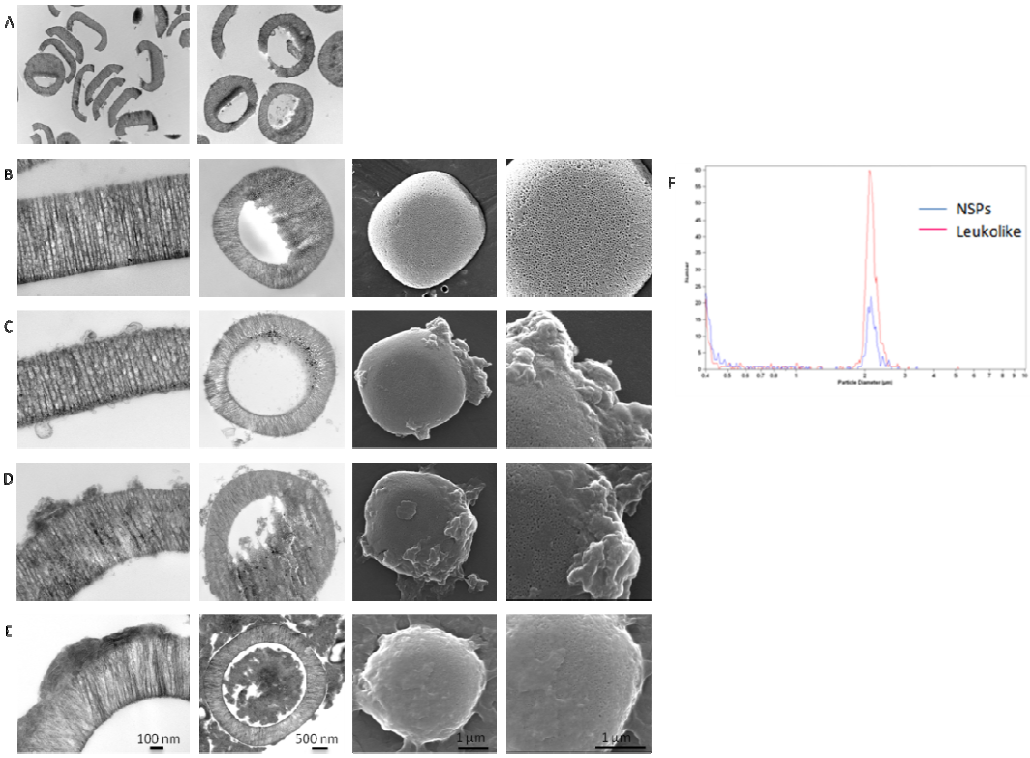

Figure 3

	Mobility	Zeta Potential (mV)	Rel Residual
Leukocyte Membranes	-1.97 ± 0.10	-26.44 ± 1.40	0.0087 ± 0.0010
Oxidized NSPs	-2.17 ± 0.19	-28.84 ± 2.49	0.0114 ± 0.0050
APTES NSPs	0.56 ± 0.09	7.41 ± 1.16	0.0064 ± 0.0010
LS	-1.70 ± 0.45	-26.00 ± 1.50	0.0102 ± 0.0051
Jurkats	-2.34 ± 0.05	-31.16 ± 0.68	0.0098 ± 0.0015

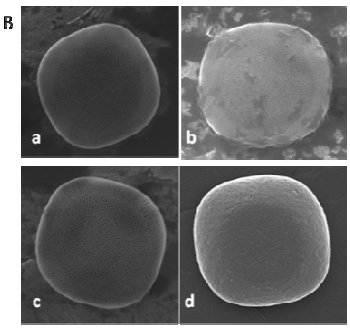

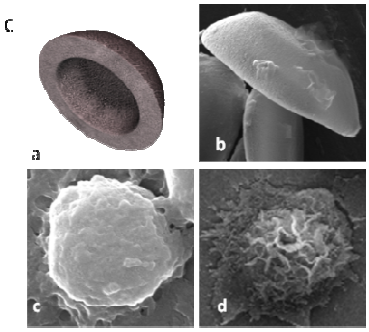

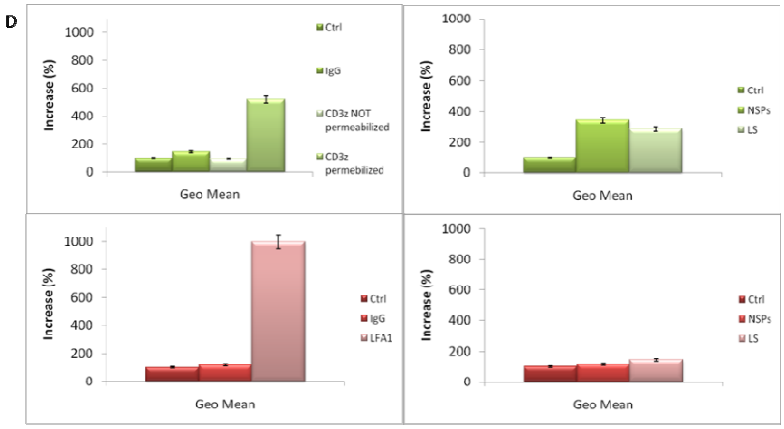

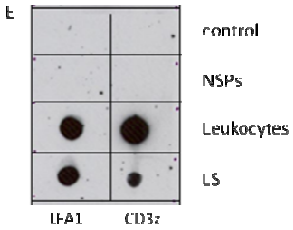

Figure 4

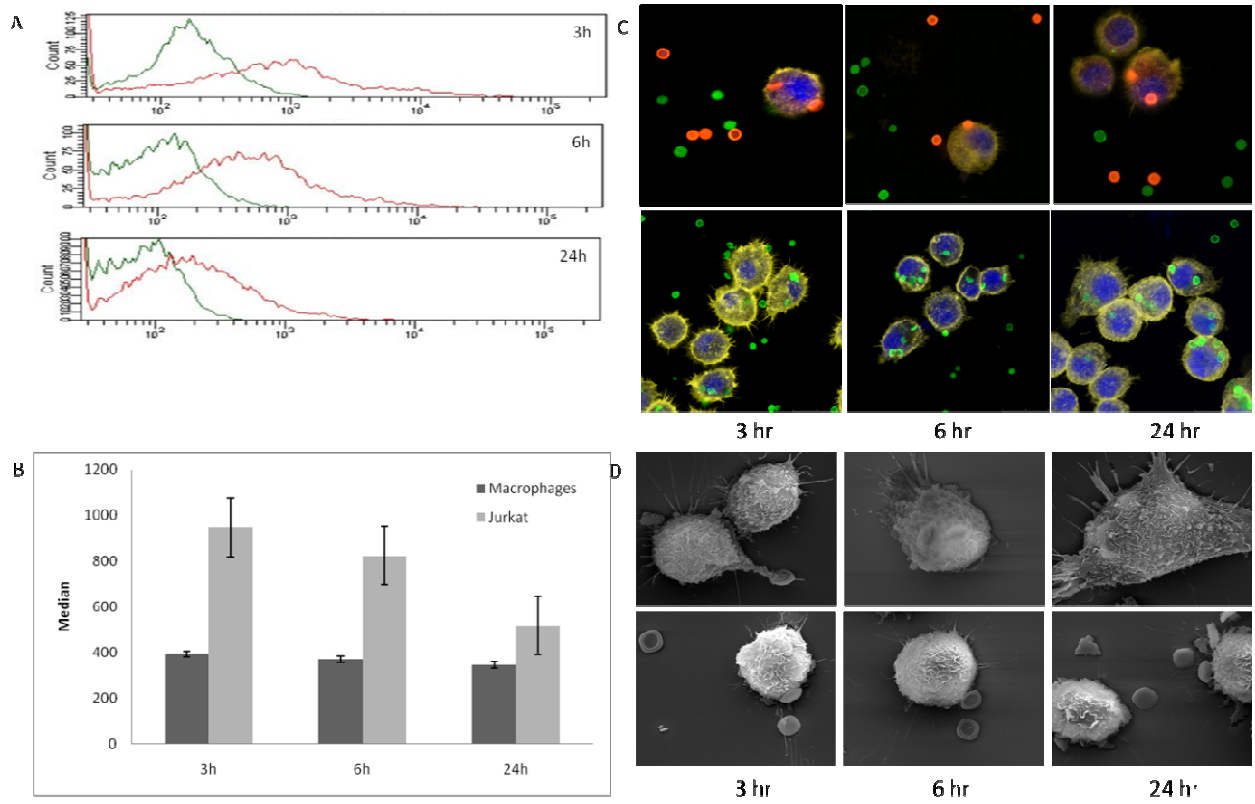
A
3h
6h
24h
Count
B
Macrophages
Jurkat
Median
1200
1000
800
600
400
200
0
3h
6h
24h
C
3 hr
6 hr
24 hr
D
3 hr
6 hr
24 hr

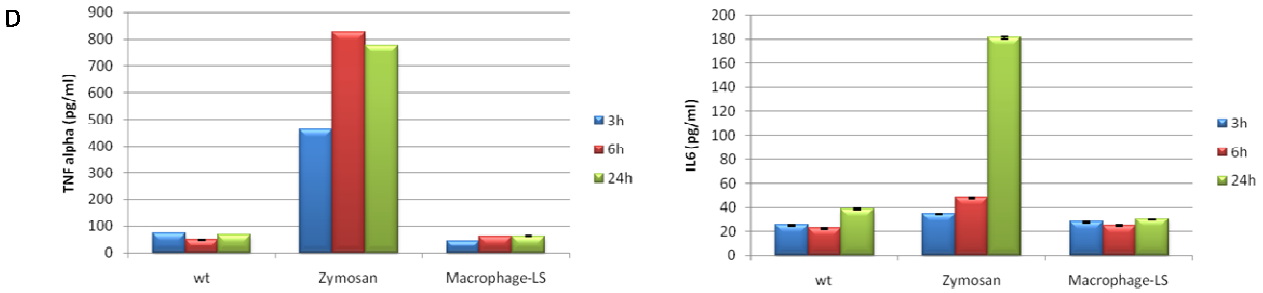
D
TNF alpha (pg/ml)
900
800
700
600
500
400
300
200
100
0
wt
Zymosan
Macrophage-LS
3h
6h
24h
IL6 (pg/ml)
200
180
160
140
120
100
80
60
40
20
0
wt
Zymosan
Macrophage-LS
3h
6h
24h

Figure 5

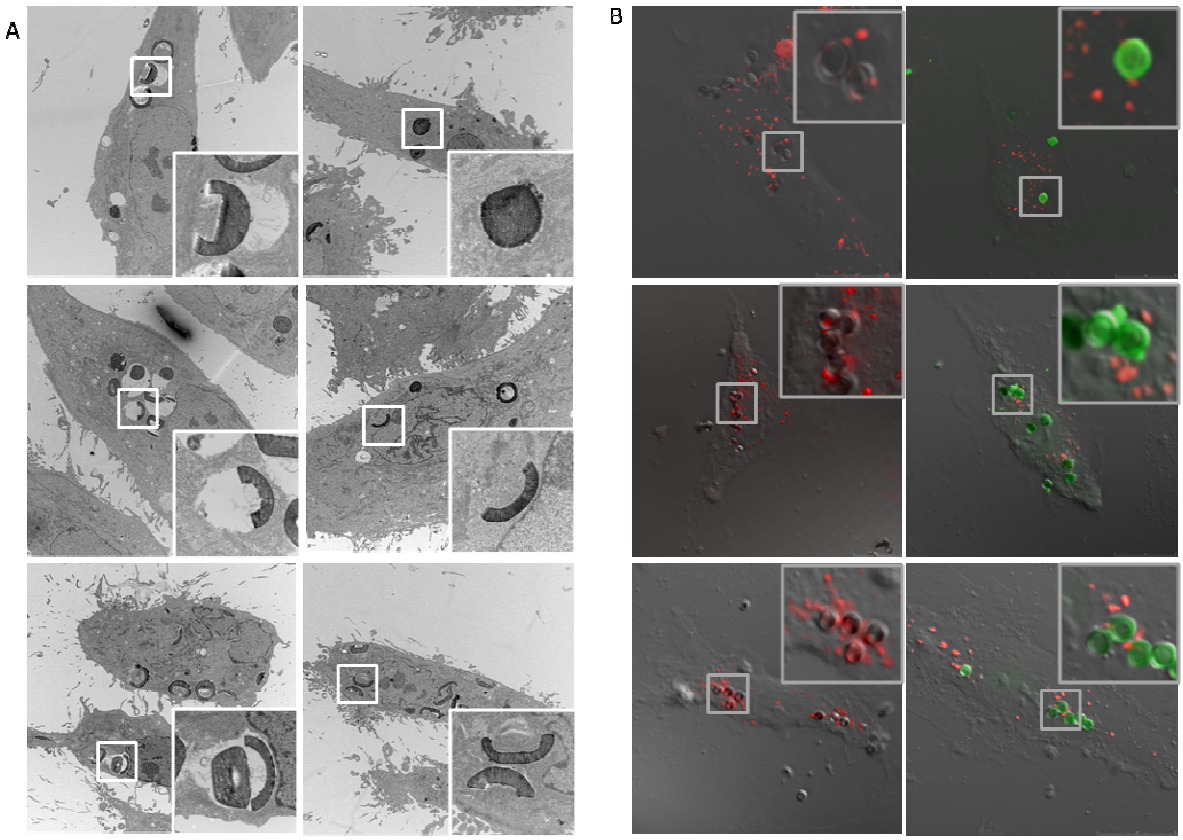

Figure 6

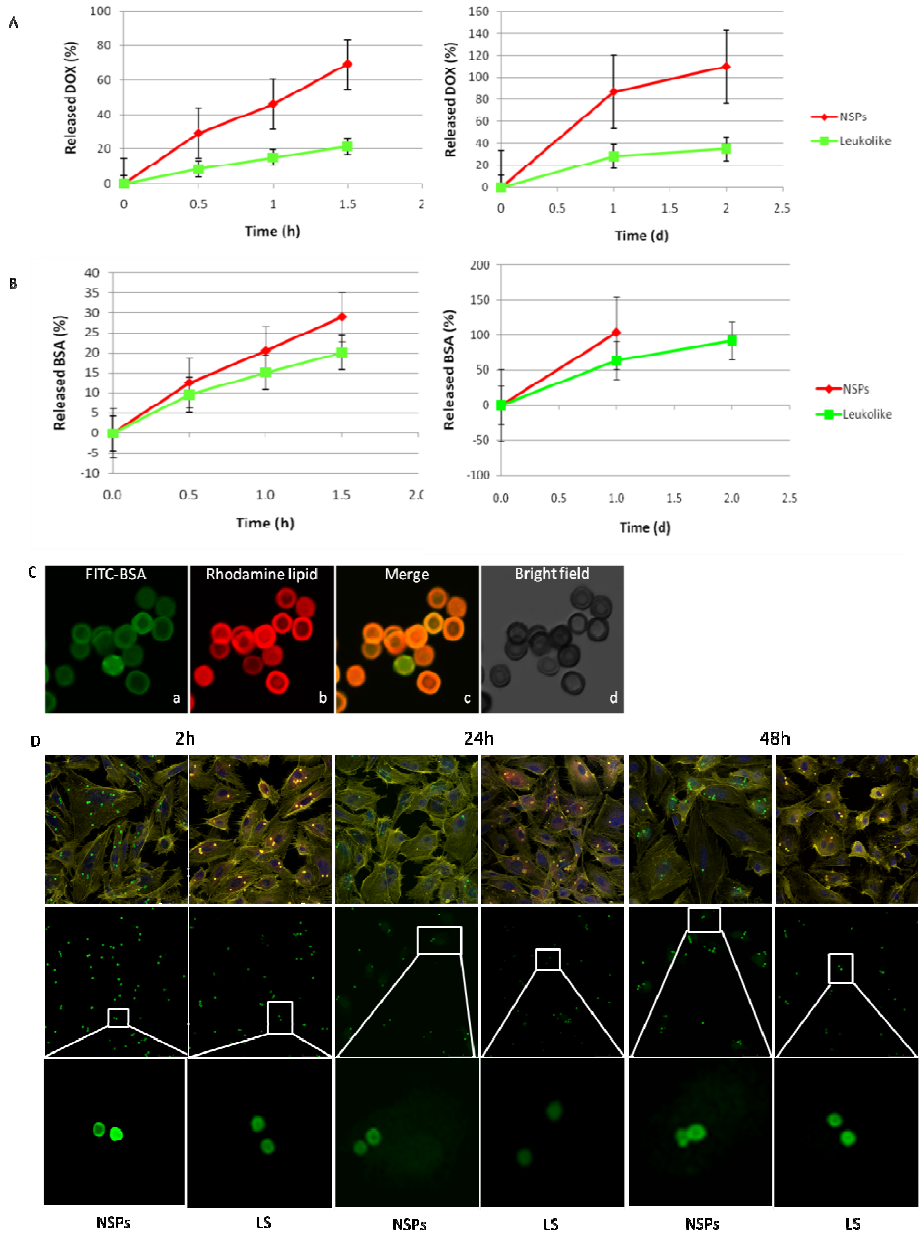
A
Released DOX (%)
Time (h)
Released DOX (%)
Time (d)
NSPs
Leukolike
B
Released BSA (%)
Time (h)
Released BSA (%)
Time (d)
NSPs
Leukolike
C
FITC-BSA
Rhodamine lipid
Merge
Bright field
a
b
c
d
D
2h
24h
48h
NSPs
LS
NSPs
LS
NSPs
LS

References

1. Ratner, B.D. and S.J. Bryant, *Biomaterials: where we have been and where we are going.* Annu Rev Biomed Eng, 2004. **6**: p. 41-75.
2. Ferrari, M., *Cancer nanotechnology: opportunities and challenges.* Nat Rev Cancer, 2005. **5**(3): p. 161-71.
3. Ferrari, M., *Nanovector therapeutics.* Curr Opin Chem Biol, 2005. **9**(4): p. 343-6.
4. Allen, T.M. and P.R. Cullis, *Drug delivery systems: entering the mainstream.* Science, 2004. **303**(5665): p. 1818-22.
5. Cho, K., et al., *Therapeutic nanoparticles for drug delivery in cancer.* Clin Cancer Res, 2008. **14**(5): p. 1310-6.
6. Moghimi, S.M., A.C. Hunter, and J.C. Murray, *Long-circulating and target-specific nanoparticles: theory to practice.* Pharmacol Rev, 2001. **53**(2): p. 283-318.
7. Ferrari, M., *Frontiers in cancer nanomedicine: directing mass transport through biological barriers.* Trends Biotechnol, 2010. **28**(4): p. 181-8.
8. Nilsson, B., et al., *Can cells and biomaterials in therapeutic medicine be shielded from innate immune recognition?* Trends in immunology, 2010. **31**(1): p. 32-38.
9. Peer, D., et al., *Nanocarriers as an emerging platform for cancer therapy.* Nat Nanotechnol, 2007. **2**(12): p. 751-60.
10. Romberg, B., W.E. Hennink, and G. Storm, *Sheddable coatings for long-circulating nanoparticles.* Pharm Res, 2008. **25**(1): p. 55-71.
11. Owens, D.E., 3rd and N.A. Peppas, *Opsonization, biodistribution, and pharmacokinetics of polymeric nanoparticles.* Int J Pharm, 2006. **307**(1): p. 93-102.
12. Ley, K., et al., *Getting to the site of inflammation: the leukocyte adhesion cascade updated.* Nat Rev Immunol, 2007. **7**(9): p. 678-89.
13. Nieminen, M., et al., *Vimentin function in lymphocyte adhesion and transcellular migration.* Nat Cell Biol, 2006. **8**(2): p. 156-62.
14. Millan, J., et al., *Lymphocyte transcellular migration occurs through recruitment of endothelial ICAM-1 to caveola- and F-actin-rich domains.* Nat Cell Biol, 2006. **8**(2): p. 113-23.

15. Nourshargh, S., P.L. Hordijk, and M. Sixt, *Breaching multiple barriers: leukocyte motility through venular walls and the interstitium.* Nat Rev Mol Cell Biol, 2010. **11**(5): p. 366-78.
16. Carman, C.V., *Mechanisms for transcellular diapedesis: probing and pathfinding by 'invadosome-like protrusions'.* J Cell Sci, 2009. **122**(Pt 17): p. 3025-35.
17. Yang, L., *ICAM-1 regulates neutrophil adhesion and transcellular migration of TNF-a-activated vascular endothelium under flow.* Blood, 2005. **106**(2): p. 584-592.
18. Azzali, G., M.L. Arcari, and G.F. Caldara, *The "mode" of lymphocyte extravasation through HEV of Peyer's patches and its role in normal homing and inflammation.* Microvasc Res, 2008. **75**(2): p. 227-37.
19. Tasciotti, E., et al., *Mesoporous silicon particles as a multistage delivery system for imaging and therapeutic applications.* Nat Nanotechnol, 2008. **3**(3): p. 151-7.
20. Decuzzi, P. and M. Ferrari, *Design maps for nanoparticles targeting the diseased microvasculature.* Biomaterials, 2008. **29**(3): p. 377-84.
21. Decuzzi, P., et al., *Size and shape effects in the biodistribution of intravascularly injected particles.* J Control Release, 2010. **141**(3): p. 320-7.
22. Chiappini, C., et al., *Tailored Porous Silicon Microparticles: Fabrication and Properties.* Chemphyschem, 2010.
23. Lee, S.Y., M. Ferrari, and P. Decuzzi, *Design of bio-mimetic particles with enhanced vascular interaction.* J Biomech, 2009. **42**(12): p. 1885-90.
24. Kalb, E., S. Frey, and L.K. Tamm, *Formation of supported planar bilayers by fusion of vesicles to supported phospholipid monolayers.* Biochim Biophys Acta, 1992. **1103**(2): p. 307-16.
25. Swanson, J.A., *Shaping cups into phagosomes and macropinosomes.* Nat Rev Mol Cell Biol, 2008. **9**(8): p. 639-49.
26. Novak, M.T., J.D. Bryers, and W.M. Reichert, *Biomimetic strategies based on viruses and bacteria for the development of immune evasive biomaterials.* Biomaterials, 2009. **30**(11): p. 1989-2005.
27. Wittchen, E.S., *Endothelial signaling in paracellular and transcellular leukocyte transmigration.* Front Biosci, 2009. **14**: p. 2522-45.

Chapter 3

CONCLUSIONS AND FUTURE PROSPECTIVES

DDS targeting perspectives

Several types of DDS have demonstrated to improve the therapeutic index of the carried drug while reducing their side effects, after intravenous administration. Although currently available DDS can enhance the drug accumulation at the interested site, especially in tumors, the DDS interactions with and uptake by the tumor cells remain insufficient. The main strategy that was proposed to further enhance drug delivery and retention at the level of tumor cells is based on the active targeting [1], that guaranties a highly specific biodistribution of the carrier due to specific interactions.

One way to promote recognition between DDS and target cells is to attach ligands at the DDS surface that can bind specifically to target cells. For instance, proteins or carbohydrates can be used as ligands of endogenous receptors expressed at the cell surface [2, 3]. An advantage of using specific ligands as targeting moieties is that the DDS would be targeted only toward cells showing high expression levels of receptors in comparison to physiological conditions. In fact, it is common in several cancer cells to observe an over-expression of some receptors, whereas other are downregulated and almost disappear from the cell surface. Thus, it seems useful to take

advantage of differences in the level of receptor expression in the targeting strategy.

However, the actual methods for grafting various types of targeting moiety on DDS surface have to be improved in order to preserve the functionality of the ligand active site.
The ideal DDS should be able to specifically target the cancer lesion while still maintaining the ability to escape the immune system and overcome all the other biological barriers.

Towards a clinical application of the Leukolike system.

According to these requests, a new efficient method for grafting targeting moieties can derive from the integration of biotechnology with immune-based and gene therapy-based approaches, which can have wide applications across the field of drug delivery.
Additionally, the combination of technology with nature in order to adapt the physiological mechanisms adopted by the immune cells to NSPs, already brought to the development of the LS a new class of DDS able to avoid unwanted uptake and clearance from RES and thereby to improve the circulation time of the first stage vectors (NSPs).
As proposed in the chapter above, the surface functionalization of NSPs with leukocyte plasma membranes can be used as a “stealth approach” to provide a physical protection against RES uptake and an increased accumulation at the tumor level with a consequent prolonged cytotoxic activity. The coating membranes, indeed, prevent

the burst release of the payload thus ensuring a prolonged activity of the drug in the time.

Thinking to an imminent test of these successful results in an *in vivo* model, eventually, it will be interesting to actively target the LS by transferring on it the natural tropism that circulating leukocytes have for the tumor site. If proved favorably, consequently, this technology will be translated to a pre-clinical model in which autologous tumor infiltrating lymphocytes (TIL) can be directly collected by biopsy of tumor samples and *ex vivo* expanded.

It is also known that after *ex vivo* expansion TIL are still able to recognize and infiltrate the tumors from which they originated [4, 5]. Moreover *ex vivo* expanded TIL still maintain markers of memory cells, co-stimulatory receptors and cell surface markers associated with their trafficking to the tumor [6]. The TIL can also be genetically modified in order to express high levels of a chimeric antigen receptor (CAR) with a particular specificity for a lineage-specific antigen of interest, that is known to be over-expressed on tumor cells.

This kind of gene-therapy approach improves the tumor-antigen phenotype of the young TIL making them and consequently the LS, an attractive solution for drug delivery because of their increased ability to specifically recognize the tumor cells.

The plasma membranes of the TIL that efficiently express CAR will be isolated and used for the realization of LS of a second generation.

By exploiting the potential of autologous TIL to migrate to the tumor microenvironment, it can be expected that the LS system, upon intravenous injection, will move toward the luminal surface of the endothelial cell drizzling the tumor mass, where will undergo

transmigration and finally accumulate in the tumor microenvironment due to the CAR tropism.

In this way, by perfectly combining the rational design of a DDS with the fundamental understanding of tumor biology, that is a necessary step to better overcome the numerous barriers encountered, the LS represents the ideal approach to determine a successful and personalized case-by-case strategy. The LS approach thus offers the possibility to create, time by time, LS with different properties able to translate a laboratory-based research into a real therapy, better suited to face the tumor heterogeneity.

The versatility of the LS, due to the natural properties of its components (autologous leukocytic membranes) and to the ability to genetically modify primary leukocytes with the desired tumor targeting agents, offers a powerful tool applicable not only to a multitude of different cancer types but to inflammatory pathologies in general.

PUBLICATIONS

Re F., Airoldi C., Zona C., Masserini M., La Ferla B., Quattrocchi N., Nicotra F., *Beta amyloid aggregation inhibitors: small molecules as candidate drugs for therapy of Alzheimer's disease*, Curr Med Chem. 2010;17(27):2990-3006.

References

1. Nobs, L., et al., *Current methods for attaching targeting ligands to liposomes and nanoparticles.* J Pharm Sci, 2004. **93**(8): p. 1980-92.
2. Gabius, H.J., *The sugar code in drug delivery.* Adv Drug Deliv Rev, 2004. **56**(4): p. 421-4.
3. Sharon, N. and H. Lis, *History of lectins: from hemagglutinins to biological recognition molecules.* Glycobiology, 2004. **14**(11): p. 53R-62R.
4. Dudley, M.E., et al., *Adoptive cell therapy for patients with metastatic melanoma: evaluation of intensive myeloablative chemoradiation preparative regimens.* J Clin Oncol, 2008. **26**(32): p. 5233-9.
5. Tran, K.Q., et al., *Minimally cultured tumor-infiltrating lymphocytes display optimal characteristics for adoptive cell therapy.* J Immunother, 2008. **31**(8): p. 742-51.
6. Powell, D.J., Jr., et al., *Transition of late-stage effector T cells to CD27+ CD28+ tumor-reactive effector memory T cells in humans after adoptive cell transfer therapy.* Blood, 2005. **105**(1): p. 241-50.